CONTENTS — A through L

GEOMORPHIC ANALYSES OF DEBRIS APRONS ALONG THE MARTIAN DICHOTOMY BOUNDARY, TEMPE TERRA/MAREOTIS FOSSAE REGION, MARS. F. C. Chuang and D. A. Crown, Planetary Science Institute, 1700 E. Fort Lowell Rd., Suite 106, Tucson, AZ 85719-2395 (e-mail: chuang@psi.edu).

Introduction. Geomorphic indicators of subsurface ice on Mars are currently the subject of intense study in the planetary community [1,2,3,4,5]. Lobate debris aprons, thick accumulations of mass-wasted material with lobate fronts, along with lineated valley fill and concentric crater fill, were first identified in regions of Martian fretted terrain along the highland-lowland boundary [6,7]. Squyres and others [6-8] postulated that features of this suite were saturated with ice and moved downslope by creep. Globally, debris aprons are found poleward of 30 N and 30 S latitude with several regions having high concentrations of these features [8]. The abundance of debris aprons along portions of the dichotomy boundary provide important clues about the types of geologic materials present in the region and the role that volatiles play in the modification of the boundary over time.

In this study, we use the abundance of new Mars orbital data to assess the geomorphic and geologic characteristics of debris aprons in the Tempe Terra/Mareotis Fossae region of Mars (43-55N, 274-294E). Comparison of apron populations from different parts of Mars will allow us to evaluate regional geologic controls and potential climatic differences on apron development.

Data and Methods. Viking, Mars Global Surveyor, and Mars Odyssey mission data were used in our analysis of debris aprons including Viking Orbiter mosaics (256 pxl/deg), gridded MOLA topography (128 pxl/deg), individual MOLA PEDR profiles, MOC narrow-angle images (2-7 m/pxl), THEMIS daytime and nighttime IR images (~100 m/pxl), THEMIS daytime VIS images (~19 m/pxl), THEMIS Brightness Temperature Record images (~ 100 m/pxl), and gridded TES thermal inertia data (~3 km/pxl). The individual datasets have been imported into ESRI ArcView 8.2 Geographic Information Systems (GIS) software for geo-registration, analysis, and generation of map products.

Regional Geology, Debris Aprons, and the Tempe/Mareotis Population. The Tempe/Mareotis study area lies along the dichotomy boundary with features typical of Martian fretted terrain [9]. Relief along the Tempe/Mareotis boundary reaches 4 km in places, particularly along escarpments to the north and northwest. The region is geologically diverse with abundant volcanic and tectonic features [10,11]. This activity, along with the possible existence of an ancient northern ocean [12,13], has resulted in the deposition of many different types of material along the dichotomy boundary. A synopsis of the Tempe/Mareotis geologic history is provided in [11].

Recent studies of lobate debris aprons have focused on two large populations, eastern Hellas and Deuteronilus Mensae [14,15,16]. Aprons at these two locations have a few similar surface textures, but are different in terms of overall size and distance from their source regions. In contrast, the aprons along the dichotomy boundary at Tempe/Mareotis and Deuteronilus have more common planimetric morphologies, morphometries, and surface textures, suggesting that these two apron populations may have similar emplacement and degradational styles compared to those elsewhere on Mars.

We have identified 65 debris aprons in the Tempe/Mareotis region using MOC, THEMIS, and Viking Orbiter images. They are typically observed as single lobes or a coalesced mass of lobes that have converged below a common source area. These aprons, like those elsewhere on Mars, are commonly found at the base of features with moderate-to- high relief such as isolated or clustered massifs, escarpments, grabens, and the interior walls of craters. The movement of debris away from the source region is generally unconfined with the exception of those within grabens. The aprons do not appear to form below any preferentially pole-facing or equator-facing slopes and are generally tens of meters thick, with a maximum of 250 m.

We have compiled statistics for all of the debris aprons in the Tempe/Mareotis population including planimetric area, maximum volume, slope, relief, and elevation range. When the population was divided into two groups, massif-related and escarpement-related, massif-related aprons were smaller in nearly every statistical category (Table 1). This difference is probably due to the fact that the higher-relief escarpments have greater surface areas from which to contribute material to debris aprons. Massifs are isolated outliers of high-standing material away from the main boundary, but have significantly less relief than escarpments. If massifs are eroded portions of highland material, one would expect these aprons to be of similar size to escarpment-related aprons. However, this is not the case and it suggests that differences in the materials along the boundary may be present.

Apron Surface Textures and Features from MOC. Four distinctive textures are observed on Tempe/Mareotis apron surfaces in narrow-angle MOC images: a) smooth, b) pitted, c) ridge and valley, and d) knobby. The textures are commonly observed along mid-to- lower apron slopes and represent different stages of preservation of the top surface.

Smooth texture. This texture represents the upper-most unmodified apron surface. The smooth surface is generally featureless with a lack of craters and erosional features. Nearly all Tempe/Mareotis aprons contain some exposure of smooth material and in some cases, the entire imaged surface of an apron has this texture.

Pitted texture. This texture is defined by individual semi-circular to elliptically-shaped pits. Smaller pits measure a few meters across, whereas larger pits have dimensions up to 135x70 m. Most pits appear to form in rows across an apron surface and multiple pits may coalesce to form one or more pit chains that can reach up to a few hundred meters in length.

Ridge and valley texture. Adjacent rows of pit chains develop an undulating topographic pattern where the linear to curvilinear depressions are valleys and the remnant materials form ridges. Ridges are generally continuous along their length, but are sometimes segmented in places. From shadow length measurements, ridges have heights of 5-35 m. The spacing between sets of ridges is often 30-90 m.

Knobby texture. The knobby texture is defined by individual or clusters of knobs that are located between low-lying degraded areas. Individual knobs typically have widths from a few tens of meters across to 100 m across. From shadow length measurements, knobs have heights up to 20 m.

Surface features. Geomorphic features observed within low-lying smooth areas include longitudinal cracks, individual and multiple broad ridges circumferential to the bases of scarps and massifs, and circular-to-sub-circular depressions.

Apron Surface Degradation Sequence. The four textures observed on apron surfaces represent different stages of progressive surface degradation. The sequence begins with an unmodified upper-most smooth surface which then develops pits. The pits coalesce to form chains and any remnant high-standing material between the depressions forms ridges. Continued degradation causes the ridges to pinch-off, forming isolated knobs that indicate a textural transition from ridge and valley to knobby. There are also cases in which a direct transition from pitted to knobby is evident. In addition, we do not find a complete degradational sequence on every apron or every part of an apron surface.

The preserved textures in this degradational sequence likely occur on an upper dust+ice mantle that overlies a lower rock+ice mixture (the main apron mass). The overlying dust+ice mantle may be the same material that has been found globally throughout the mid-to- high latitudes (30-70 N) of Mars [17]. The dissected appearance of this global 1-10 m thick mantling layer is morphologically similar to our pitted and ridge and valley textures.

We attribute the surfaces of Tempe/Mareotis debris aprons to degradation by a combination of ice sublimation, melting of ice, and eolian activity. Ice contained within the mantle is most likely lost by sublimation, which forms an irregular surface exposing more of the internal ice to the atmosphere. Warming from seasonal changes could melt pockets of subsurface ice, forming voids that causes surface collapse and the eventual formation of pits. This process is analogous to the formation of thermokarst in periglacial regions on Earth, but on Mars thermokarst might be "dry" given the instability of liquid water under current atmospheric conditions [16,18].

Following the initial step of pit formation by surface collapse, ice sublimation could cause widening of the pits and the development of low-lying valleys or large depressions. As sublimation continues, remnant fine-grained material that collects on the walls and floors of pits may build-up to form a lag deposit. If sufficiently thick, the lag could arrest the sublimation process. However, if eolian activity in the area is sufficiently strong to lift and transport particles away, sublimation could then continue to further degrade the apron.

Table 1. Statistics of the Tempe/Mareotis apron population

	Total	Massif-related	Escarpment-related
Area[1]	12-2303	12-716	90-2303
Volume[2]	0.5-1327	0.5-180	28-1327
Relief[3]	0.01-1.8	0.01-1.45	0.33-1.8

[1] sq. kilometers [2] cu. kilometers [3] kilometers

References. [1] Malin M.C. and Edgett K.S. (2001) *JGR, 106,* 23429-23570. [2] Costard et al. (2002) *Science, 295,* 100-113. [3] Christensen P.R. (2003) *Nature, 422,* 45-48. [4] Milliken et al. (2003) *JGR, 108,* 11-1 to 11-13. [5] Head et al. (2003), *Nature 426,* 799-802. [6] Squyres S.W. (1979) *JGR, 84,* 8087–8096. [7] Squyres S.W. et al. (1992) *Mars, Univ. of AZ Press,* 523-554. [8] Squyres S.W. and Carr M.H. (1986) *Science, 231,* 249-252. [9] Sharp, R.P. (1973) *JGR, 78,* 4073-4083. [10] Hodges C.A. and Moore H.J. (1992) *USGS, Prof. Paper #1592*. [11] Moore H.J. (2001) *USGS, Misc. Invest. Series Map I-2727*. [12] Parker T.J. et al. (1989) *Icarus, 82,* 111-145. [13] Parker T.J. et al. (1993) *JGR, 98,* 11061-11078. [14] Pierce T.L. and Crown D.A. (2003) *Icarus,163,* 46-65. [15] Mangold N. and Allemand P. (2001) *GRL, 28,* 407-410. [16] Mangold N.A. (2003) *JGR, 108,* 2-1 to 2-13. [17] Mustard J.F. et al. (2001) *Nature, 412,* 411-414. [18] Costard F.M. and Kargel J.S. (1995) *Icarus, 114,* 93-112.

MARS CRUSTAL DICHOTOMY AND WORLD MAPS WITH CONSTANT SCALE NATURAL BOUNDARIES (CSNB)

"A creative approach to visualizing subtle points of geodesy." [8]

C. S. Clark, architect, 1100 Alta Avenue, Atlanta, Georgia 30307; rightbasicbuilding@yahoo.com

Introduction: It has long been known that world maps with natural boundaries have an advantage-in-principle over world maps without [3], because the mind is clouded by meaningless interruptions.

World maps with constant scale natural boundaries (CSNB) improves things because in it [6] [7], peripheries are not grossly distorted in shape, and map edges become recognizable places--a comprehensible overall view boosting scientific intuition [5] [9].

Context is clear in a CSNB map and, if boundaries well-chosen, clearer still, even on complex planets as Earth (see Fig. 6) and, Figures 1 and 4, Mars.

Other contexts for viewing Mars crustal dichotomy in CSNB are identified.

Mapping Précis: Begin at Valles Marineris and proceed downstream where, if Mars as Earth had "switched on" tectonically, we might find to map a linear system of basaltic magmatism [2]. Instead, we find a multi-legged dry-bed, the bottom of a "hill" [4], nether regions of Mars crustal dichotomy. See Fig. 1.

Other Mapping Précis: A "dales"-centered CSNB map (Fig. 4 inside out) would show lowlands as a single, watershed-edged basin, with Mars' continental divide as its perimeter boundary [4]. {POSTER}

And, a lowlands ridge-edged map, uplands still map midst like Fig. 4, would preserve on the map as sensible districts, at the expense of lowland peninsulas, the much-studied outflow channels [1]. {POSTER}

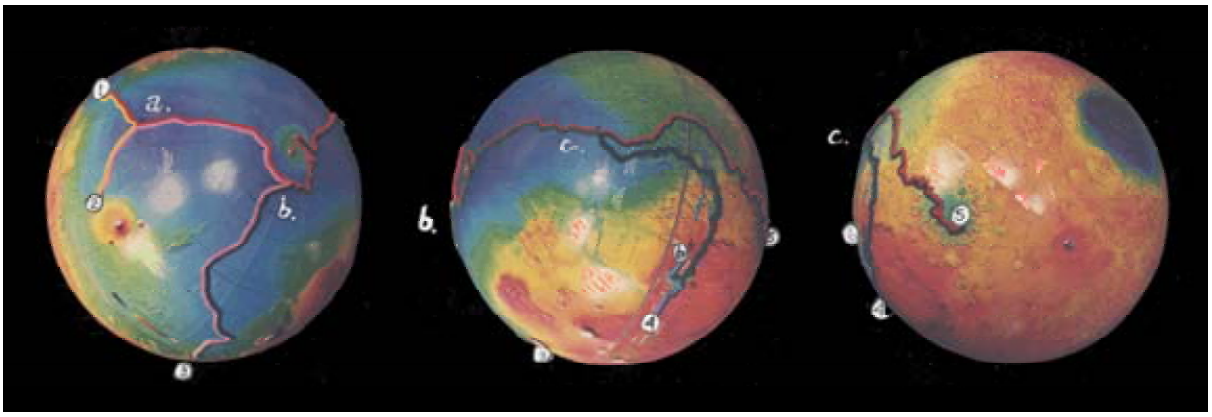

FIGURE 1: False color topo Mars globe marking dry-beds, the extremities of a single "hill" [4]. Commonly mapped Figure 2, this pattern may also be plotted as a CSNB map, Figures 3 and 4.

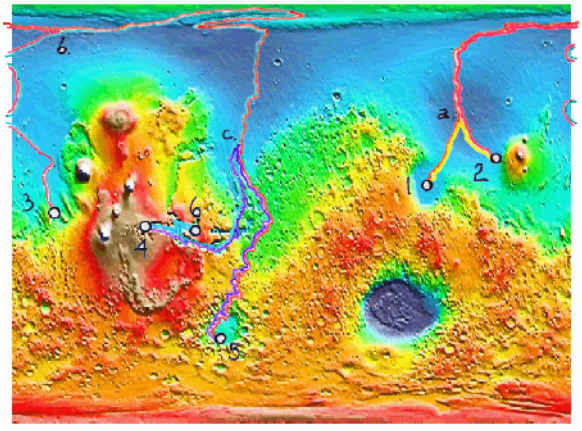

FIGURE 2: Dry-beds on a conventional Mars map. Note polar contortions and longitudinal interruption.

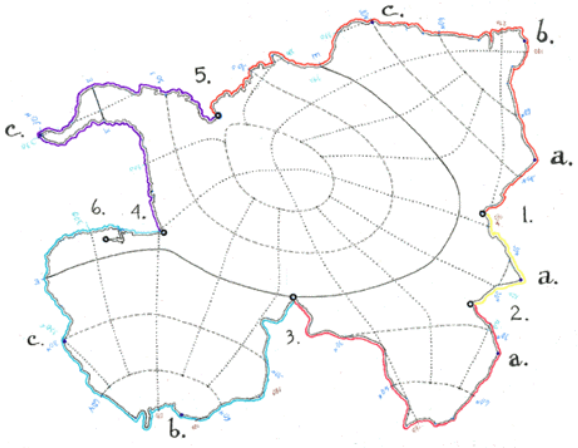

FIGURE 3: Mars dry-beds edging a CSNB map; a coarse calculus preserves their shapes [6]. See Fig. 4.

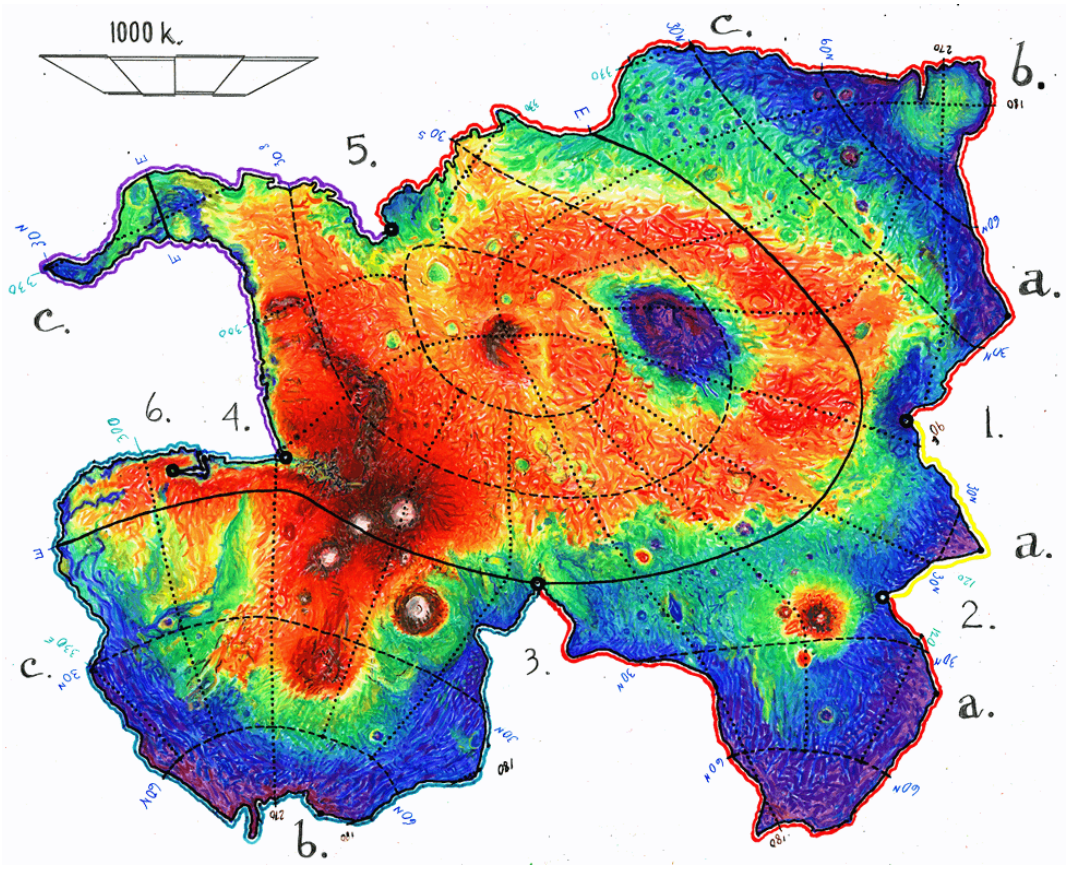

FIGURE 4: A world map of Mars edged by lowlands, its youngest crust. Compare Figure 2. It may surprise planetary scientists that a map's borders may be fruitfully entertained; compare also Figure 6.

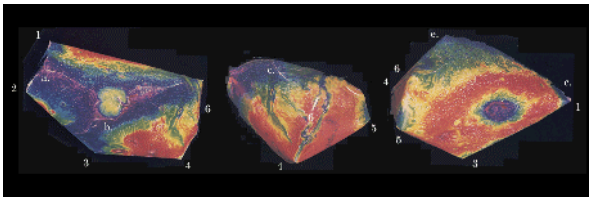

FIGURE 5: CSNB map folds to a condensed-sphere model; a unique solid, unobtainable without CSNB and, happily, a check on mapmaker's accuracy.

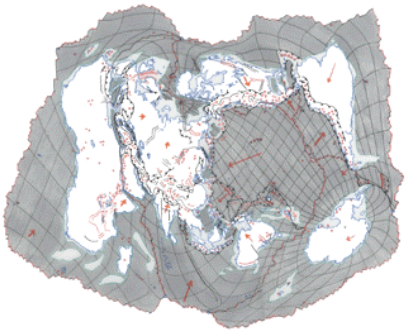

FIGURE 6: Earth, in a CSNB map edged by a portion (slowest moving) of its youngest crust.

References: [1] Carr M. H. (2000) *SPC* **The Surface of Mars** 11, 12. [2] Lowman P. D. (2002) *CUP* **Exploring Space, Exploring Earth** 254, 265. [3] Spilhaus A. F. and Snyder J. P. (1991) *CGIS-ACSM* 18 4 World Maps with Natural Boundaries. [4] Maxwell J. C. (1870) *Phil. Mag.* 40 269 On Hills and Dales. [5] Clark C. S. (2004) *NCGT News.* Illustrating Concepts in Global Tectonics with 'CSNB.' [6] Clark C. S. (2003) *ISPRS WG-IV/9* Visual Calculus or Perceptual Fribble? 'CSNB' A Novel Projection Method, Well-Suited to Our Era. [7] Clark C. S. (2002) *LPS XXXIII* #1794 'CSNB' and the Asteroid Eros. [8] Krantz S. K. (2003) *comment*--Krantz is former chair. of math. at Wash. U. St. L. [9] Morse, H. C. M. (1950) *manu. Kenyon Coll.* The Poet and Reality: a conf. in honor of Robert Frost/Some Reflections on Evaluations in Mathematics and the Arts, also *(1959) Bull. Atom. Sci. XV 2* and *(2004) MAA* **Musings of the Masters** Mathematics and the Arts.

A MAGNETIC PERSPECTIVE ON THE MARTIAN CRUSTAL DICHOTOMY. J. E. P. Connerney[1], M. H. Acuna[1], N. F. Ness[2], D. L. Mitchell[3], R. P. Lin[3], and H. Reme[4], [1]NASA Goddard Space Flight Center, Code 695, Greenbelt, MD 20771; Connerney@gsfc.nasa.gov, [2]University of Delaware, Newark, DE 19716, [3]Space Science Laboratory and Physics Department, University of California, Berkeley, CA, 94720.

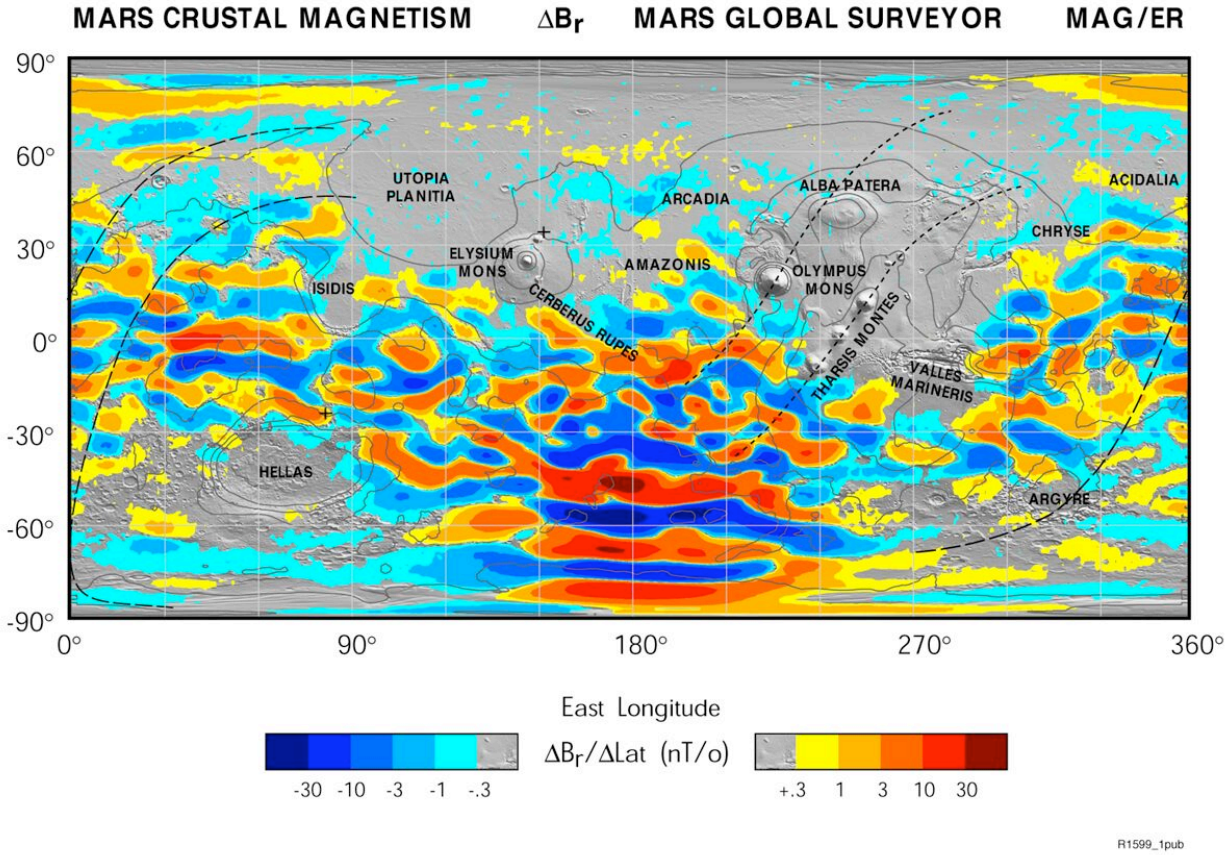

Introduction: The Mars Global Surveyor spacecraft has completed two Mars years in nearly circular polar orbit at a nominal altitude of 400 km. The Mars crust is at least an order of magnitude more intensely magnetized than that of the Earth [1], and intriguing in both its global distribution and geometric properties [2,3]. Measurements of the vector magnetic field have been used to map the magnetic field of crustal origin to high accuracy [4,5]. This most recent map is assembled from > 2 full years of MGS night-side observations, and uses along-track filtering to greatly reduce noise due to external field variations.

The map: The radial field component was averaged along-track and decimated to 1 sample per degree latitude traversed by MGS in its polar orbit. A simple 3-point non-recursive digital filter (differentiating Lanczos filter) is then applied to the time series to attenuate constant offsets and variations of larger spatial scale than those associated with variations of crustal magnetization. We then take the median value of all points falling in each 1 by 1 degree bin in latitude and longitude to create a global image of the field. The resulting map has about an order of magnitude greater sensitivity to crustal magnetic fields. This map of the *change* in radial field with latitude (dBr/dTheta) is closely related to a map of the theta component of the field, with the added advantage of superior removal of external fields.

Overview: The crustal demagnetization previously associated [2] with the large impact basins (Hellas, Argyre, Utopia, Isidis) is even more obvious in this new map, as is the crustal demagnetization associated with the large volcanic structures (Tharsis, Olympus Mons, Elysium). A number of geologic features previously identified in imagery and topography (Cerberus Rupes, Valles Marineris) now can be seen to have magnetic signatures as well. Lack of magnetization seems to be associated with emplacement of lavas.

Crustal magnetization extends well beyond the older Noachian southern highlands terrain. We suggest that the smooth, flat northern lowlands are underlain by much older crust, an extension of the southern highlands crust. This is consistent with the inferred Noachian age of the underlying crust based on the detection of "Quasi-circular depressions", thought to be buried craters [6]. Much of the crustal magnetization originally imprinted in the underlying crust may have been erased by thermal remagnetization in a weak field (after the demise of the dynamo) following the catastrophic widespread emplacement of a ~1 km thick volcanic layer throughout the northern lowlands [7]. If so, a low temperature magnetic mineralogy (titanomagnetite, magnetite) is implicated and the magnetic layer must be relatively thin, e.g., few km in thickness.

Plate tectonics: Another kind of fault, not previously recognized in imagery or topography, can be identified in the Meridiani region by inspection of the magnetic contours. Two long dashed lines are superposed on the map to identify the location of the proposed faults, along which the magnetic field pattern appears to shift. These lines are drawn by rotation of a vector about a common axis of rotation identified by a pole (marked with a cross) located at 23º S and 80.5º E, just north of Hellas. The magnetic imprint is best preserved near 0º latitude and 0º longitude, where the map shows a series of east-west trending features of alternating polarity extending from ~15º N to ~30º S. A similar pattern can be found on either side of the proposed fault lines. The magnetic imprint has been altered where the crust has been reworked by impacts (e.g., the multi-ring crater Ladon near 18º S, 331º E) and perhaps other events. The two proposed parallel great faults are separated by ~1400 km and a similar pattern in the magnetic field is found on both sides of the easternmost fault along ~2700 km of its length.

The magnetic imprint in Meridiani is consistent with crust formed by plate tectonics in the presence of a reversing dynamo. Essential characteristics: (1) a magnetic imprint aligned with the ridge axis or spreading center, (2) a comparable magnetic imprint observed at widely separated locations, and (3) the presence of transform faults, or great faults, along which relative plate motion has occurred. The relative motion of two rigid plates on the surface of a sphere may be described as a rotation about an axis. If two plates have as common boundaries a number of great faults, they must lie on small circles about the rotation pole. The great faults in Meridiani define an axis of rotation (23º S and 80.5º E) describing the relative motion of two ancient plates, north and south of the equator. The ~240 km offset of the putative ridge axis in Meridiani is comparable to that observed along ocean ridges on Earth.

The origin of the great Valles Marineris fault system is controversial, but it has been attributed to planetary rifting [8] and compared to terrestrial plate tectonic rifts, e.g., the east African rift zone. A rift structure of parallel grabens and troughs forms, often along an arc, where the crust is being pulled apart by tensile forces. The west-northwest trend of Valles Marineris is oriented nearly perpendicular to the direction of plate motion implied by the great faults in Meridiani (relative plate motion occurs along the strike of transform faults). The direction of tensile forces required to form Valles Marineris, if it is a rift structure, is consistent with the motions implied by the proposed transform faults in Meridiani.

The great volcanic edifices of the Tharsis Montes (Arsia Mons, Pavonis Mons, Ascraeus Mons, extended to include Ceraunius Tholus/Uranius Patera and volcanic cones in Tempe Terra) and the pair Olympus Mons, Alba Patera lie nearly on two small circles (short dashed lines) about a common axis (through 35.5º N and 152º E). The motion of a single plate over a pair of mantle hotspots in a direction parallel to the dashed lines could form a chain of volcanoes if the magma source periodically breached the crust (e.g., the Hawaiian island chain of volcanoes in the Pacific). The relative ages assigned to these volcanoes is consistent with plate motion northward over a pair of putative mantle hotspots, with Alba Patera and Uranius Patera forming early, Olympus Mons and Arsia Mons later.

Dichotomy boundary: The dichotomy boundary is a reflection of crustal evolution, following (from Isidis to Tharsis south of Elysium and Lucas Planum) a series of relic transform faults and spreading centers [9], elsewhere defined by catastrophic lava flows encroaching upon highlands terrain. The Mars crust reflects the end of an era of plate tectonics, a relic of crustal spreading, rifting, plate motions, and widespread volcanism following the demise of the dynamo.

References:

[1] Acuna, M. H., et al., 1998, *Science,* 279, 1676 – 1680.

[2] Acuna, M. H., et al., 1999, *Science*, 284, 790 – 793.

[3] Connerney, J. E. P., et al., 1999, *Science*, 284, 794 – 798.

[4] Connerney, J. E. P., et al., 2001, *Geophys. Res. Lett.*, 28, 4015 – 4018.

[5] Connerney, J. E. P., et al., 2004, *Science*, submitted.

[6] Frey, H. V., et al., 2002, *Geophys. Res. Lett.* , 29, 10.1029/2001GL013832.

[7] Head, J. W., III et al., 2002, J. Geophys. Res., 107, 10.1029/2000JE001445.

[8] Hartmann, W. K., 1973, *Icarus* 19, 550-575; Blasius, K. R., et al., 1977, *J. Geophys. Res.* 82, 4067-4091; Frey, H. V., 1979, *Icarus* 37, 142-155.

[9] Sleep, N. H., 1994, *J. Geophys. Res*, 99, 5639-5655.

ANCIENT GIANT BASIN/AQUIFER SYSTEM IN THE ARABIA REGION, MARS, AND ITS INFLUENCE ON THE EVOLUTION OF THE HIGHLAND-LOWLAND BOUNDARY

J.M. Dohm[1], N.G. Barlow[2], Jean-Pierre Williams[3], J.C. Ferris[4], H. Miyamoto[5,6], V.R. Baker[1,5], W.V. Boynton[5], R.G. Strom[5], Alexis Rodríguez[7], Alberto G. Fairén[8], Trent M. Hare[9], R.C. Anderson[10], J. Keller[5], K. Kerry[5], [1]Department of Hydrology and Water Resources, University of Arizona, Tucson, AZ, 85721, jmd@hwr.arizona.edu, [2]Dept. Physics and Astronomy, Northern Arizona University, Flagstaff, AZ, 86011, [3]Dept. of Earth and Space Sciences, Univ. of California, CA 90095, [4]U.S. Geological Survey, Denver, CO, 80225, [5]Lunar and Planetary Laboratory, University of Arizona, Tucson, AZ, [6]Department of Geosystem Engineering, University of Tokyo, [7]Department of Earth and Planetary Science, University of Tokyo, 7-3-1 Hongo, Bunkyo-ku Tokyo 113-0033, Japan, [8]Centro de Biología Molecular, Universidad Autónoma de Madrid, 28049 Cantoblanco, Madrid, Spain, [9]U.S. Geological Survey, Flagstaff, AZ, 86001, [10]Jet Propulsion Laboratory, Pasadena, CA.

Introduction: Ancient geologic and hydrologic phenomena on Mars observed through the magnetic data [1,2] provide windows to the ancient past through the younger Argyre and Hellas impacts [e.g.,3,4], the northern plains basement and the rock materials that mantle the basement [e.g.,5,6], and the Tharsis and Elysium magmatic complexes (recently referred to as superplumes [7,8]). These signatures, coupled with highly degraded macrostructures (tectonic features that are tens to thousands of kilometers long [9]), reflect an energetic planet during its embryonic development (0.5 Ga or so of activity) with an active dynamo and magnetosphere [1,2,6]. One such window into the ancient past occurs northwest of the Hellas impact basin in Arabia Terra. Arabia Terra is one of the few water-rich equatorial regions of Mars, as indicated through impact crater [10] and elemental [11,12] information. This region records many unique characteristics, including predominately Noachian materials, a highland-lowland boundary region that is distinct from other boundary regions, the presence of very few macrostructures when compared to the rest of the cratered highlands, the largest region of fretted terrain on Mars, outflow channels such as Mamers Valles that do not have obvious origins, and distinct albedo, thermal inertia, gravity, magnetic, and elemental signatures [13]. We interpret these to collectively indicate a possible ancient giant impact basin that later became an important aquifer, as it (1) provides yet another source of water for the formation of putative water bodies that occupied the northern plains [14,15], (2) helps explain possible water-related characteristics that may be observed at the Opportunity landing site, (3) identifies a potential contributor to the development of the long-lived Tharsis superplume [7,8], and (4) provides a viable explanation for the unique character of the highland-lowland boundary when compared to other boundary regions of Mars. This primary basin is approximately antipodal to Tharsis and estimated to be at least 3,000 km in diameter (see Fig. 1a,b of [13]).

Discussion: Collectively, the distinct characteristics of Arabia Terra add credence to the following proposed hypothesized sequence of events (from oldest to youngest): (1) an enormous ancient impact basin at least 1.5 times the size of Hellas forms during extremely ancient Mars when the dynamo is active and the lithosphere is relatively thin, (2) sediments and other materials infill the basin during high erosion rates and a productive Noachian aquifer system is established, (3) the basin isostatically adjusts, (4) uplift of basin materials related to the growth of antipodal Tharsis results in differential erosion, exposing ancient stratigraphic sequences, and (5) parts of the ancient basin/aquifer system remain water-enriched [13].

The putative Arabia impact basin should not be unexpected on Mars. During the earliest period of solar system history some 4.2 billion years ago, there were very large impacts on the Moon and terrestrial planets. Impact basins comparable in size and age occur on the Moon. The largest impact basin ever identified is the Procellarum basin, first discovered by Whitaker [16] and confirmed from Lunar Prospector chemical data by Feldman et al. [17]. Based on structural and elemental information, the manifestation of the extremely large impact event recorded on the lunar surface extends for an estimated radius of about 60° or a diameter of about 3600 km. Feldman, et al [17] present evidence, which includes elemental information, of yet another giant impact basin on the lunar far side with a radius of 50° or about 3000 km diameter. Both of these basins have also been heavily cratered by the period of late heavy bombardment as the Arabia basin. The South Pole-Aitken basin (2500 km diameter) is another example of a heavily cratered large basin on the Moon. On Mercury, there is also an old giant impact basin (Borealis Basin) with an estimated diameter of 1500 km, but only 25% of that planet has been observed at sun angles sufficient to detect old basins. Even larger basins may occur on the unexplored side. The surface of Venus is too young to record such extremely large impact basins, and on

Earth the earliest part of solar system history is not preserved.

An old impact basin the size of the putative Arabia should, in fact, be present on Mars. The primary impact basin proposed for the Arabia Terra region is estimated to be at least 3,000 km in diameter, or at least 1.5 the size of Hellas. However, its total deformational extent may approximate or even exceed the estimated total extent of the Procellarum impact event. Whether the proposed Arabia Terra impact basin included multi-ring structures and associated basins is difficult to ascertain due to the observed high degree of erosion and deformation of the region.

Although we do not know how much water the Arabia impact basin/aquifer held, we can get some idea by estimating the water content for a 5 kilometer-thick layer coincident with an approximated 3000 km diameter. The volume of such a layer is about 1.43×10^7 km^3. If the porosity was about 10% then the total volume of water would have been about 1.4×10^6 km^3. This is comparable to about 10% of the volume of the smallest ocean in the Northern Plains based on the interior shoreline dimensions of [15,18]. However, this estimated volume may be much higher if the basin had a greater depth and total extent.

Implications: Implications of the basin hypothesis include: (1) explaining the unique characteristics of the region, (2) providing another source of water for the putative water bodies that occupied the northern plains [15,19-20], (3) providing additional information to assess the water-related characteristics observed at the Opportunity landing site, (4) identifying a potential contributor to the development of the long-lived Tharsis superplume [7-8], and (5) providing a viable explanation for the unique character of the highland-lowland boundary when compared to other boundary regions of Mars.. Furthermore, the existence of an ancient, gigantic basin in the Arabia terra region, especially when taken in conjunction with the smaller yet massive Tharsis basin [21], suggests that rapid obscuration of basins (be they tectonic or impact in origin) and infill with volatile-rich materials was a relatively common phenomena early in martian history. This has profound implications for rates of deposition in the earliest of martian times, and alludes to an environment with vigorous geomorphic processes being driven by a dynamic hydrosphere. The Arabia terra basin also brings into focus the timing of formation for the northern lowlands. Although this manuscript suggests that the formation of the highland-lowland boundary postdates the formation and infilling of the Arabia terra basin, several investigators have suggested that the dichotomy was shaped by geophysical phenomena present as the planet cooled and first formed a crust, such as mantle convection associated with core formation [22]. If so, why were the northern lowlands not also infilled by materials and therefore obscured to the present day? Were rates of deposition somehow different for the polar regions, or was the mechanism that formed the northern plains and global dichotomy longer-lasting, perhaps related to incipient plate tectonism [6-7,9,23]? Although many questions are still left to be answered, the emerging picture is that the topography of extremely ancient Mars was drastically different from what is observed today. In addition, such geologic information should provide the constraints on theoretical models relating to the time-space relations of the formation of the highland-lowland boundary, including geophysical modeling of the planet's interior.

References: [1] Acuna M. H. et al. (2001) *JGR*, 106, 23,403-23,417. [2] Arkani-Hamed, Jafar (2003) JGR, 108, 10.1029/2003JE002049. [3] Scott, D.H. and Tanaka, K.L. (1986) *USGS I-Map 1802A*. [4] Greeley, Ronald, and Guest, J.E. (1987) *USGS I-Map 1802B*. [5] Frey, H.V. et al. (2002) Geophys. Res. Lett. 29, 10.1029/2001GL013832. [6] Fairén, A.G. and Dohm, J.M. (2004) *Icarus*, 168, 277-284, 2004. [7] Baker, V.R. et al. (2002) A theory of early plate tectonics and subsequent long-term superplume activity on Mars. Electronic Geosciences 7, (<http://lin.springer.de/service/journals/10069/free/conferen/superplu/>), 2002. [8] Dohm, J.M., et al. (2002a) *Superplume International Workshop*, Abstracts with Programs, Tokyo, 406-410, 2002. [9] Dohm, J.M., et al. (2002b) *Lunar Planet. Sci. Conf.,* XXXIII, #1639. [10] Barlow N.G. and Perez, C.B. (2003) *JGR, 108*, 10.1029/2002JE002036. [11] Boynton W.V. et al. (2002) *Science, 297*, 81-85 [12] Feldman W.C. et al. (2002) *Science, 297*, 75-78. [13] Dohm, J.M., et al. (2004) *Lunar Planet. Sci. Conf.,* XXXV, #1209. [14] Baker, V. R. (2001) *Nature*, 412, 228-236. [15] Fairén, A.G., et al. (2003) *Icarus*, 165, 53-67. [16] Whitaker, E.A. (1981) *Proc. Lunar Planet. Sci.* 12A, 105-111. [17] Feldman, W.C., et al. (2002) *J. Geophys. Res.*, 107, E3, 10.d29/2001JE001506, 2002. [18] Ormo, Jens, et al. (2004) Meteoritics & Planetary Science, 39, 333-346. [19] Parker, T.J., et al. (1987) in *Symposium on Mars: Evolution of its Climate and Atmosphere, LPI Tech. Rept. 87-01*, 96-98. [20] Baker, V.R., et al. (1991) *Nature*, 352, 589-594. [21] Dohm, J.M., et al. (2001) *J. Geophys. Res*. 106, 32,943-32,958, 2001. [22] Wise, D.U., et al. (1979) *Icarus*, 38, 456-472. [23] Fairén, A.G., et al. (2002). Icarus 160, 220-223.

MARTIAN EARLY MAGNETIC FIELD AS A RESULT OF MAGMA OCEAN CUMULATE OVERTURN. L.T. Elkins-Tanton, S. Zaranek, and E.M. Parmentier, Department of Geological Sciences, Brown University, Providence, RI 02912 (Linda_Elkins_Tanton@brown.edu, Sarah_Zaranek@brown.edu, EM_Parmentier@brown.edu).

Introduction: Dynamical models of Martian differentiation and early evolution need to be consistent with several major attributes of Mars that are believed to have developed before 4.0 Ga: differentiation of mantle source regions into isotopically distinct reservoirs; development of an early, brief, strong magnetic field; and the formation of an early crust to record that field. Significant and perhaps complete melting of the large terrestrial planets is expected due to the conversion of kinetic energy to heat during accretion of planetesimals, and to the potential energy release of core formation [e.g., 1-5]. Previous results of Martian magma ocean investigations indicated that magma ocean crystallization and subsequent overturn on Mars could be fast and complete [6], and is consistent with magma source region differentiation and the development of an alumina-poor Martian mantle [7]. The further results presented here demonstrate that magma ocean crystallization and overturn can produce a magnetic field of between 10 and 50 million years duration.

Magma ocean model: The fundamental, relevant processes of cooling to the liquidus of the magma ocean, crystallizing between the liquidus and solidus, crystal setting, and convection are well summarized in Solomatov [8]. Vigorous convection in the low viscosity liquid magma ocean is assumed to result in an adiabatic variation of temperature with depth. As the liquid magma ocean cools by the loss of heat convected to the surface of the planet, the adiabat first intersects the liquidus at the bottom of the mantle. As the ocean continues to cool a partially solid region develops at the bottom of the mantle.

The simplified Martian mantle mineralogy used here follows from the bulk mantle composition of Bertka and Fei [9] and the phase relations of Longhi *et al* [10]. All phases are fractionally crystallized in increments of one-half percent from the evolving liquids of the magma ocean. One percent of interstitial liquid is retained in the solids throughout the magma ocean, acting as a reservoir for radiogenic incompatible elements, which are partitioned from the solid phases using coefficients from [11-13]. Major and trace element liquid and solid compositions are tracked throughout the crystallization process.

As crystallization progresses the solids remain at their solidus temperatures, but the temperature of the solidus decreases as liquid composition evolves. The final cumulate stratigraphy, lying at its solidus, ranges in temperature from 2,100°C at the core-mantle boundary to about 700°C near the surface.

The resulting cumulate stratigraphy is unstable to gravitational overturn mainly due to the effects of iron enrichment as fractional solidification proceeds. Because the time scale for Rayleigh-Taylor overturn is inversely dependent upon the thickness of the layer, overturn is not likely to initiate until the magma ocean is largely crystalline, whereupon the cumulates flow as solids into an equilibrium density profile [7]. A more detailed description of this model is available in the companion abstract in this volume and in Elkins-Tanton *et al.* [7].

Core heat flux model: Because cumulate overturn is expected to occur on a time scale significantly less than that of heat conduction, the core-mantle boundary will effectively remain at its pre-overturn temperature during and immediately after overturn. The density profile of the solidified magma ocean predicts the stratigraphy of the overturned cumulates, from which the temperature profile directly follows since the solids move adiabatically during the rapid reshuffling. Moving cold cumulates from near the surface to the core-mantle boundary during overturn can produce a brief and intense heat flow out of the hot core and into the cold cumulates.

A finite difference computer program in spherical coordinates has been written to predict heat flux from the core by solving the conductive heat equation while incorporating conductive cooling at the top of the mantle, cumulate heating from incompatible radiogenic elements (whose distribution is produced by the initial fractional crystallization of the magma ocean), and the initial temperature distribution in the overturned cumulates. No convection is allowed in this model; the stable density profile created by cumulate overturn should prevent initiation of convection on these time scales.

Stevenson [14] estimates that a superadiabatic core cooling rate on the order of 80K per Ga (corresponding to about 0.022 J/m^{2}sec) is required to initiate a Martian core dynamo. Our calculations indicate that a minimum superadiabatic heat flux from the core required to initiate a dynamo may be as high as 0.11 J/m^{2}sec, but is likely between 0.05 and 0.02 J/m^{2}sec, using equation 3 from [14].

Results for core heat flow following cumulate overturn: Assuming that the Martian silicate mantle begins with a chondritic trace element composition, the final one percent of liquid contains a trace element concentration of about 65 times chondritic, similar to bulk Earth crust (fig. 1). An evolved liquid fraction is spread over a radius of about 250 km by a critical crystal network and possible stagnant crust at the surface of the planet. Some portion of this ~700°C material falls during overturn to the core-mantle boundary, which remains at the silicate solidus temperature of about 2,100°C, carrying with it U, Th, and K concentrations that will produce significant heating. The falling layer is sufficiently thick that even a stagnant lid on

the planet will not prevent some quantity of cold radiogenic material from foundering. Core heat flux is therefore driven by the initial steep temperature gradient between the core and the cold fallen cumulates, but increasingly limited both by core cooling and by radiogenic heating in the lowermost cumulates.

All the models in this suite produced a final cumulate overturn stratigraphy where the coolest, shallowest cumulates fell to the core-mantle boundary. (Results from [7] showed the garnet layer falling to the core-mantle boundary, but the more evolved liquid compositions allowed in these more sophisticated models prevent complete fall of the garnet layer in every case.) The preferred initial temperature difference across the core-mantle boundary is therefore 2,100-700°C = 1,400°C (fig. 2).

If the temperature difference is 1,400°C, heat flux from the core begins at about 0.6 J/m^{2}sec, dropping off exponentially and falling below 0.05 J/m^{2}sec about 50 million years later (fig. 3). In this model the Martian core therefore has sufficient superadiabatic heat flux to initiate a core dynamo for about 50 million years after magma ocean crystallization, as shown in figure 2. Over this period the core cools by about 80 degrees.

If the temperature difference across the core-mantle boundary is only 1,000°C, heat flux remains above the necessary 0.05 J/m^{2}sec for about 30 Ma. To prevent core heat flux from ever exceeding the 0.05 J/m^{2}sec value the temperature difference across the core-mantle boundary must be 150°C or less.

Discussion and Conclusions: All the models run in this suite produced superadiabatic core heat flux thought to be sufficient to produce a core dynamo magnetic field for at least 30 to 50 million years after magma ocean cumulate overturn. Overturning cumulates moves cold cumulates to the core-mantle boundary, producing core heat flux, and also moves hot cumulates nearer the surface, where they can melt adiabatically and produce an early crust. These models predict the formation of tens of kilometers of new crust during the time the magnetic field is active. This new crust is at the surface at temperatures cooling to and then below the Curie temperature of approximately 600°C, available to record the magnetic field.

References: [1] Safronov (1978) *Icarus 33*, 3. [2] Kaula (1979) *JGR 84*, 999. [3] Stevenson (1987) *Ann. Rev. EPS 15*, 271. [4] Halliday (2001) *Space Sci. Rev 96*, 197. [5] Hess (2001) *32nd LPSC*, 1319. [6] Zaranek (2004) *35th LPSC*. [7] Elkins-Tanton (2003) *MAPS 38*, 1753. [8] Solomatov (2000) in *Origin of the Earth and Moon*. [9] Bertka (1997) *JGR 102*, 5251. [10] Longhi (1992) In *Mars*. [11] Draper (2003) *PEPI 139*, 149. [12] Green (2000) *Lithos 53*, 165. [13] Skulski (1994) *Chem. Geo. 117*, 127. [14] Stevenson (2003) *EPSL 208*, 1.

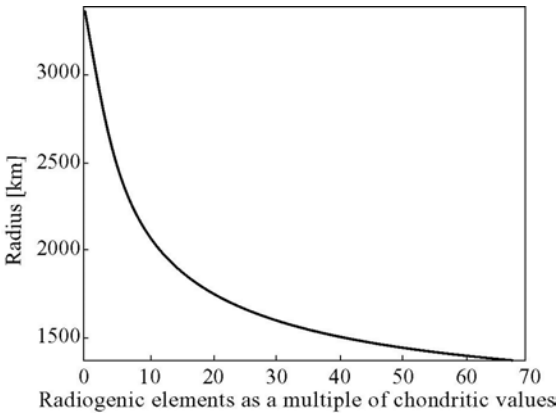

Figure 1. Profile of radiogenic trace elements immediately following cumulate overturn, as a multiple of chondritic values.

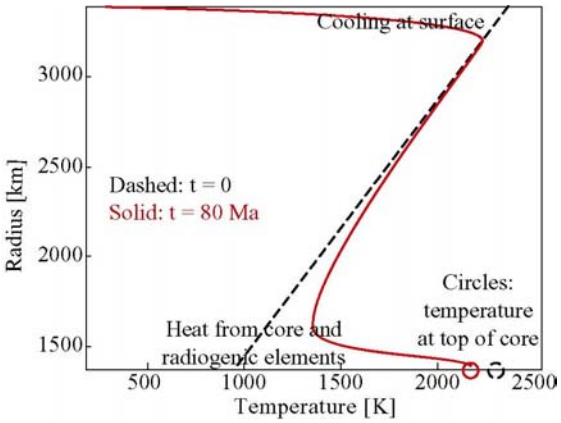

Figure 2. Temperature profiles through the Martian mantle immediately following overturn, and at 80 Ma, approximately 30 Ma after cessation of the Martian magnetic field in these models.

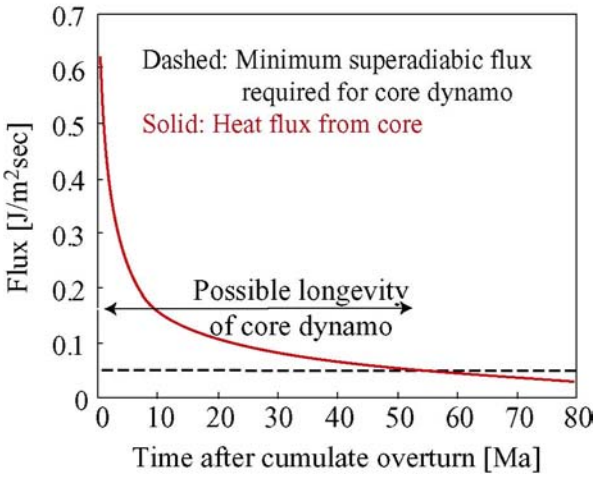

Figure 3. Heat flux from the Martian core following magma ocean cumulate overturn. Heat flux values above about 0.05 J/m^{2}sec (horizontal dashed line) should be sufficient to produce a core dynamo.

MAGNETIC ANOMALIES NORTH OF THE DICHOTOMY BOUNDARY: POSSIBLE EVIDENCE FOR DICHOTOMY RETREAT? C. I. Fassett[1] and J. W. Head III[1], [1]Dept. of Geological Sciences, Brown University (Caleb_Fassett@brown.edu & James_Head@Brown.edu).

Introduction: The Mars Global Surveyor magnetometer experiment revealed strong crustal magnetic anomalies, predominately in the southern highlands [1]. It is generally believed that these anomalies were emplaced quite early in Mars' history given the apparent demagnetization of the major impact basins [1]. Besides the correspondence of the major basins with regions of low magnetism and the broad difference between hemispheres, there are relatively few correlations between the crustal magnetic signature and other geological features.

A particular region of interest where remanent magnetism is poorly correlated with geology is observed near the dichotomy boundary, especially in the region from 60º to 160º E (Fig. 1, modified from [2]). A magnetic signature appears to extend at least 500 km north from the present dichotomy. At present, we are attempting to understand the implications that this observation may have for helping to unravel the complicated history of the dichotomy boundary, as well as for understanding of the magnetic anomalies and their modification history. In what follows, we briefly outline several possible models.

Erosion and Retreat of the Dichotomy Boundary: One possible interpretation of this observation is that the magnetic signature observed north of the dichotomy may be a sign of widespread and substantial retreat of the dichotomy itself. In this model, the magnetic anomalies north of the dichotomy boundary act as a tracer for old highlands crust that was subsequently eroded and perhaps partially buried by younger volcanism. Widespread backward erosion (on the order of hundreds of kilometers) of the dichotomy boundary has been suggested before based upon geological evidence [3]. Moreover, the location of these anomalies (and their formation by erosion of highland crust) appears to be somewhat consistent with the Hb1 (Hesperian boundary plains 1) unit mapped by Tanaka et al. [4].

The simplest model for erosional retreat of several hundred kilometers is water-associated erosion; groundwater sapping, fluvial erosion, ice-related mass-wasting, or glaciation may all have played a role. This widespread removal of material is consistent with the formation of the knobby terrain spottily distributed north of and adjacent to the dichotomy boundary (HNk in [4]). Erosion would presumably have predominantly occurred in the Noachian and early Hesperian, when the dichotomy boundary may have intersected with the ancient groundwater table [5] and when erosion rates on Mars were higher [6].

Northern Lowlands Demagnetization and Formation: Another possible explanation for the magnetic anomalies that lie north of the present dichotomy boundary is that they represent northern lowlands crust which has not lost its magnetization. A clear mechanism for demagnetizing the northern lowlands remains uncertain, although the emplacement of volcanic plains appears to be insufficient. More promising is demagnetization related to a large impact (or impacts) which may have formed the northern lowlands [7] or from hydrothermal activity postdating lowland formation [8]. If the northern plains formed via one or several large impacts, it is unclear why the margins of such an impact would not be demagnetized; however, our understanding of the nature of such a large impact (and its thermal and shock effects on remanent magnetization) are presently rather limited. Alternatively, if hydrothermal demagnetization was the dominant reason for the lack of magnetic anomalies in the northern lowlands, the degree of demagnetization might decrease around the edges, because as elevation increases it is possible that groundwater availability might be decreased.

Edge Effect: A final possibility is that the observed magnetic anomalies near the dichotomy boundary might simply represent an edge effect caused by the contrasting regions of magnetized highlands and demagnetized lowlands crust [e.g., 9]. Although we are attempting to model such an effect, and have not yet ruled such a possibility out completely, it seems somewhat unlikely that this effect would produce features of the wavelength and magnitude seen here; this is especially true given the limited edge effects seen on the boundaries of other demagnetized regions, such as Hellas.

Summary and Future Work: The crustal magnetic signature adjacent to and north of the dichotomy boundary provides a potential constraint on the boundary's geological evolution. Although we need to explore alternative hypotheses more fully, we believe that this magnetic signature plausibly supports the model that the ancient dichotomy boundary was substantially north of its present location [3].

References: [1] Acuña, M.H. et al. (1999) *Science*, 284, 790-793. [2] Connerney, J.E.P. et al. (2001), *GRL*, 28, 4015-4018. [3] Tanaka, K.L. & Scott, D.H. (1987), *U.S.G.S. Misc. Inv. Series Map I-1802-C*. [4] Tanaka, K.L. et al. (2003), *JGR*, 108, 8043. [5] Head, J.W. et al. (2004), *LPSC XXXV* abstract no. 1379. [6] Craddock, R.A. & Maxwell, T.A., (1993) *JGR*, 98, 3453-3468. [7] Wilhelms, D.E. & Squyres, S.W. (1984), *Nature*, 309, 138-140. [8] Solomon, S.C. et al. (2003), *LPSC XXXIV*, abstract no. 1382. [9] Smrekar, S.E. et al. (2002), *LPSC XXXIII*, abstract no. 2068.

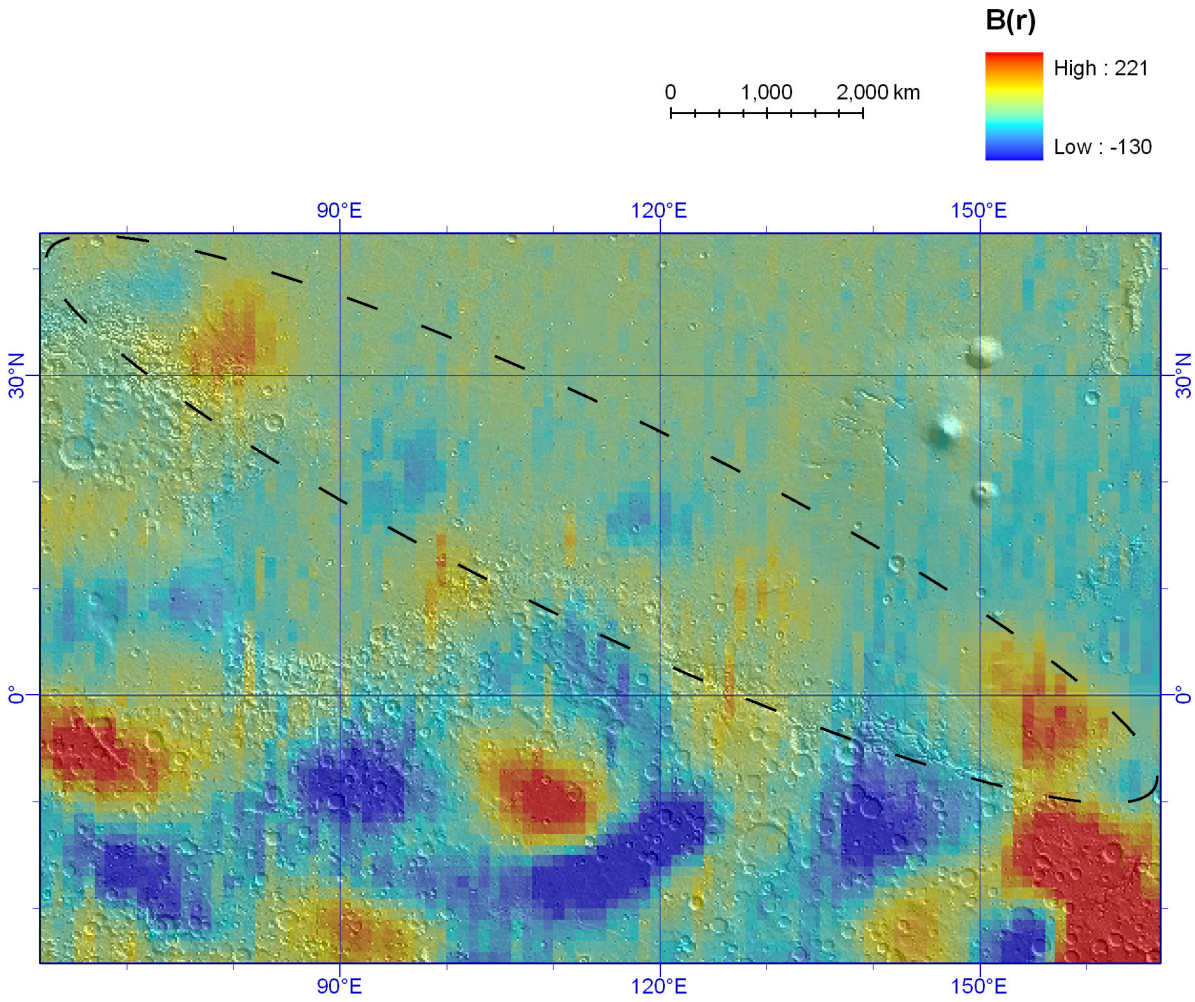

Figure 1. MGS radial magnetic measurement at 400 km modified from [2], superposed upon MOLA shaded relief. The data is stretched to bring out the weak features north of the dichotomy boundary. The relative weak signal is consistent with removal of magnetized crust during retreat of the dichotomy, though this is not a unique explanation. Magnetic anomalies extend ~500 km from the dichotomy boundary. In parts of this region, knobby terrain (HNk) appears to be correlated with the magnetic signature (e.g. 80°E, 32°N).

IMPACT CONSTRAINTS ON THE AGE AND ORIGIN OF THE CRUSTAL DICHOTOMY ON MARS.

H.V. Frey, Geodynamics Branch, Goddard Space Flight Center, Greenbelt, MD 20771; Herbert.V.Frey@nasa.gov.

Introduction: MOLA data have revealed a large population of "Quasi-Circular Depressions" (QCDs) with little or no visible expression in image data. These likely buried impact basins [1,2] have important implications for the age of the lowland crust, how that compares with original highland crust, and when and how the crustal dichotomy may have formed [3-6]. The buried lowlands are of Early Noachian age, likely slightly younger than the buried highlands but older than the exposed (visible) highland surface. A depopulation of large visible basins at diameters 800 to 1300 km suggests some global scale event early in martian history, maybe related to the formation of the lowlands and/or the development of Tharsis. A suggested early disappearance of the global magnetic field can be placed within a temporal sequence of formation of the very largest impact basins. The global field appears to have disappeared at about the time the lowlands formed. It seems likely the topographic crustal dichotomy was produced very early in martian history by processes which operated very quickly. This and the preservation of large relic impact basins in the northern hemisphere, which themselves can account for the lowland topopgraphy, suggest that large impacts played the major role in the origin Mars' fundamental crustal feature.

QCDs > 200 km Diameter: Figure 1 shows polar views of QCDs > 200 km diameter. Features of this size, which number >500, are difficult to bury completely (rim heights 1-1.5 km, depths ~4 km [7]) and therefore might be expected to survive over all of martian history. This is also a size appropriate for comparison with gravity and magnetic anomalies [8-11].

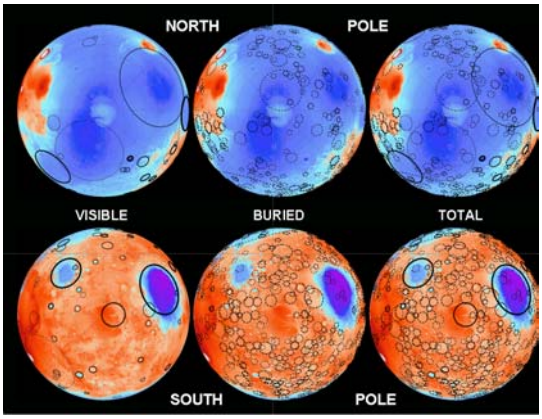

Figure 1: Polar views of visible, buried and total (= visible + buried) QCDs > 200 km diameter. Note the larger number of buried basins in both hemispheres, and the larger total number in the south.

In both highlands and lowlands the buried population is always much greater than the visible population. There is a significant number of very large basins (D>1000km), equally divided between the two hemispheres, including two Utopia-size buried highland features. One is near but not identical to an earlier proposed "Daedalia Basin" [12,13] and the other centered near 4N, 16W. This "Ares" basin may have influenced early fluvial drainage through the Uzboi-Ladon-Arden Valles and Margaritifer-Iani Chaos depressions.

Cumulative Frequency Curves and Crater Retention Ages: A small (~10) population of very large basins (D=1300-3000km) follow a –2 power law slope on the log-log cumulative frequency plots. At D < ~500 km the total populations in both highlands and lowlands again follow a –2 slope; for the planet-wide visible population this is the same slope as for the very large diameter basins. The relative positions of the lowland and highland curves indicate the buried lowland crust is slightly younger than the original (now buried) highland crust, consistent with our earlier result [2]. By direct comparison with the oldest exposed surface units on Mars (Nh_1, SE of Hellas [3,4]), the buried lowland crust is Early Noachian in age [14].

At intermediate diameters (1300 to about 800 km) the global visible population falls off the –2 slope before recovering at smaller diameters. This depletion of intermediate size basins may be the signature of some global-scale event very early in martian history. Candidates include formation of the slightly younger lowland crust (i.e., the formation of the topographic crustal dichotomy), and the growth of Tharsis (or both), both of which could have removed pre-existing intermediate-size basins.

Implications for the Age and Origin of the Crustal Dichotomy: Unless there is some way to preserve the large population of Early Noachian (now buried) impact craters while lowering the crust in the northern third of Mars, it appears the lowland crust not only formed in the Early Noachian but also became low during that time [2,14]. The slight crater age difference (which could be a very short absolute time interval), does suggest the lowlands formed after the highlands were in place and preserving craters. It may be hard to form the lowlands by endogenic processes in the short time available. Most mechanisms suggested [15-17] have a relatively late formation of the lowlands. Even if degree one convection does occur, it appears to take hundreds of millions of years to become established, even with extreme viscosity gradients [17]. How much longer, and by what exact means,

the crust then becomes low, is generally discussed in only vague terms. In contrast, three large "lowland-making" QCDs (Utopia, Acidalia and Chryse) do account for most of the lowland topography and offer a simple impact mechanism for the early formation of a topographic dichotomy on Mars [18].

Comparison with Magnetic Anomalies: We compared the distribution of QCDs (both buried and visible) with the distribution of magnetic anomalies [9,10,19-21]. Only the two oldest very large basins, Daedalia and Ares, have prominent anomalies lying within their main rings. Daedalia and Ares likely predate the disappearance of the global magnetic field. The "lowland-making" basins Utopia, Acidalia and Chryse have only a few moderate amplitude anomalies within their main rings, and are of intermediate age between Ares and the younger Hellas, Argyre and Isidis basins (see below). The demise of the global magnetic field may have been at about the time of formation of these "lowland-making" basins.

A Chronology of Major Events in the Early History of Mars: We used the cumulative number of basins larger than 200 km diameter per million square km [N(200)] to place the large diameter basins in a relative chronology [6, 18, 22]. The N(200) relative crater retention ages can be converted into "absolute ages" [22,23] using the Hartmann-Neukum (H&N) model chronology [24]. This is uncertain by at least a factor 2 [25]. We use Tanaka's [26] crater counts at small diameters (2, 5, 16 km) to convert his N(16) ages for major epoch boundaries (Early Noachian/Middle Noachian [EN/MN], etc.) to N(200) ages assuming a -2 power law. Hartmann and Neukum [24] give a model absolute age for each of these epoch boundaries. We consider two cases for the H&N value for the earliest age we find, extrapolated from the large basin population (D>1300 km diameter): a linear extrapolation from the EN/MN and MN/LN points and the unlikely case that the origin of Mars at 4.6 BYA is the upper limit.

Table 1 shows the resulting N(200) and "absolute ages" in billions of Hartmann-Neukum years for major events in martian history. With the factor of 2 and an additional pre-Noachian crater saturation caveat, the buried highlands are slightly younger (4.08-4.27) than the Ares Basin (4.09-4.28), and distinctly older than the buried lowlands at 4.01-4.11 BY. These buried lowlands are slightly younger than the "lowland-making" basins Utopia, Acidalia and Chryse at 4.04-4.20 BY, as they should be. We take this to be the age of the formation of the crustal dichotomy. This is also close to the time when the global magnetic field died, based on which basins do and do not have anomalies within their main rings. It may be that the two events, formation of the fundamental crustal dichotomy and the demise of the global magnetic field, are related.

Table 1. A Proposed N(200) Time-Line for the Early Crustal Evolution of Mars

N(200)	Feature	Event	Epoch	H/N Age
~0.1	Visible Lowlands		EH	3.65
0.16	EH / LN BOUNDARY		EH/LN	3.70
~0.6	Visible Highlands		LN/MN	3.79
0.64	LN / MN BOUNDARY		LN/MN	3.80
1.28	MN / EN BOUNDARY		MN/EN	3.92
~1.3	Isidis	Impact	EN	3.92
~2.2	Argyre	Impact	EN	4.00-4.07
~2.5	Buried Lowlands		EN	4.01-4.11
~2.7	Hellas	Impact	EN	4.02-4.14
3.0-3.2	Chryse, Utopia, Acidalia	Lowlands formed?		4.04-4.20
~3.5?		Core Field Dies?		4.07-4.23
~3.8	Buried Highlands		pre-N	4.08-4.27
~4.0	Ares	Impact	pre-N	4.09-4.28
~4.5	Total Highlands		pre-N	4.10-4.33
~8.5	Large Basin Highlands (ext)	Impacts	pre-N	4.20-4.60

Conclusions: The (visible and buried) large diameter crater population suggest the buried lowlands are slightly younger than the buried highlands, but significantly older than the exposed highland surface. The buried lowland crust is Early Noachian in age and the lowlands likely formed by processes that operated relatively quickly. In a Hartmann-Neukum model chronology, a crustal dichotomy produced by large "lowland-making" impact basins formed by 4.12 +/- 0.08 BYA and the global magnetic field died at about or slightly before the same time (4.15 +/- 0.08 BYA).

References. [1] Frey, H. et al., GRL 26, 1657-1660, 1999. [2] Frey, H. et al., GRL 29, 10.1029 /2001 GL013832, 2002. [3] Frey, E.L. and H.V. Frey, AGU Paper P32A-01. [4] Frey, H. et al., LPSC 34 abstract #1848, 2003. [5] Frey, H., GSA Fall 2002 Meeting paper 26-3, 2002. [6] Frey, H. LPSC 34, abstract # 1838, 2003. [7] Garvin, J.B. et al. LPSC 33, abstract 1255, 2002. [8] Smith, D.E. et al., Science 286, 94-97, 1999. [9] Acuna, M.H., et al., Science 284, 790-793, 1999. [10] Connerney, J.E.P. et al., GRL 28, 4015-4018, 2001. [11] Frey, H. LPSC 35, abstract #1384, 2004. [12] Craddock, R.A. et al., JGR 95, 10729-10741, 1990. [13] Schultz, R. A. and H.V. Frey, JGR 95, 14,175-14,189,1990. [14] Frey, H. et al. LPSC abstract #1680, 2002. [15] Wise, D.U. et al., JGR 84, 7934-7939, 1979. [16] McGill, G.E. and A.M. Dimitriou, JGR 95, 12595-12605, 1990. [17] Zhong, S. and M.T. Zuber, Earth Planet. Sci. Letrt. 189,75-84,2001. [18] Frey, H. 6th Intern. Coll. On Mars, abst #3104, 2003. [19] Purucker, M.E. et al., GRL 27, 2449-2452, 2000. [20] Cain, J. unpublished data, 2001. [21] Langlais, B. JGR 10.1029/2003JE002048, 2003. [22] Frey, H., GSA Fall 2003 Meeting, paper 67-5, 2003. [23] Frey, H., LPSC35, abstract #1382, 2004. [24] Hartmann, W.K. and G. Neukum, Space Sci. Rev., 96, 1-30, 2001. [25] Hartmann, W.K., personal communication, 2002. [26] Tanaka, K. L et al., Chap. 11 in *Mars*, Kieffer et al. (ed.), 1992.

CONSTRAINTS ON EARLY MARS EVOLUTION AND DICHOTOMY ORIGIN FROM RELAXATION MODELING OF DICHOTOMY BOUNDARY IN THE ISMENIUS REGION. A. Guest[1] and S. E. Smrekar[1], [1]Jet Propulsion Laboratory, California Institute of Technology, M.S. 183-501, 4800 Oak Grove Dr. Pasadena, CA 91109; alice.guest@jpl.nasa.gov.

Introduction: The Martian dichotomy is a global feature separating the northern and southern hemispheres. The 3.5-4 Gyr old feature [1,2] is manifested by a topographic difference of 2-6 km and crustal thickness difference of ~15-30 km between the two hemispheres [3,4,5]. In the Ismenius region, sections of the boundary are characterized by a single scarp with a slope of ~ 20°-23° and are believed to be among the most well preserved parts of the dichotomy boundary. The origin of the dichotomy is unknown. Endogenic hypotheses do not predict the steep slopes (scarps) of the dichotomy boudndary. Exogenic models for forming the northern lowlands by impact cratering, associate the scarps along the dichotomy boundary with craters' rims [6], but are not globally consistent with the topography and gravity [5]. In order to better understand the origin of the Martian dichotomy, it is necessary to know if the steep scarps along the boundary represent the original shape of the dichotomy.

Smrekar et al. [7] presented evidence showing that the boundary scarp in Ismenius is a fault along which the highland crust was down faulted [8]. We test whether the relaxation process could produce faulting along the dichotomy boundary and examine the crustal and mantle conditions that would allow for faulting to occur within 1 Gyr and preserve the long wavelength topography over another 3 Gyr. We approach the problem by a combination of numerical and semi-analytical modeling. We test different viscosity profiles and crustal thicknesses by comparing our modeled magnitude, location and timing of plastic strain and displacements to detailed geologic observations in the Ismenius region.

Previous Works: Nimmo and Stevenson [9] modeled relaxation of the Martian dichotomy. They argue that the topographic boundary is not relaxed and that the boundary can be preserved for a crustal thickness of 80 km or less. Their model uses viscous rheology, assumes a dry diabase flow law [10], and compares the predicted topographic relaxation to 10 evenly spaced (excluding Tharsis) profiles across the dichotomy, averaged along track. The focus of their study was on constraining crustal thickness and the amount of crustal heat production.

Numerical Model: We construct a visco-elasto-plastic finite-element model to predict the relaxation of the topography over time. The model is 1500 km wide and 1000 km deep, and consists of two materials, the crust and the mantle. We test two different crustal thicknesses (35, 80 km) and a plateau elevation 5 km. The width of the dichotomy boundary is 143 km and the average slope, smoothed using a cosine function is 2°. Assuming a crustal density of 2900 kg/m3, a mantle density of 3500 kg/m3, we include a 24.17 km thick crustal root below the plateau to produce an isostatic compensation [10]. In the equation, the total strain is defined as a sum of elastic, viscous and plastic strains [11]. We use wet diabase [10] and wet dunite [12] as a representative for the creep strain of the crust and mantle, respectively. We use a Mohr-Coulomb criterion for plasticity, with cohesion of 9 MPa and friction of 40°. The temeperature in our model is represented by an error function connecting a surface temperature of 220 K, a tempeture 1400 K (assumed to be the base of the lithosphere) at 60 km depth, which gives a thermal gradient of ~20 K/km, and a mantle temperature 1600 K or 2150 K.

Semi-analytical Model: Assuming an incompressible viscous fluid, the equilibrium and constitutive equations can be solved semi-analytically in the frequency domain [13]. The horizontal variations of the stress and velocity are transformed using a FFT allowing us to numerically integrate the equilibrium and constitutive equations only along the vertical axis. The vertical velocity at the surface is then converted to the change of topography over time. The numerical integration allows for variations of viscosity with depth. The viscosity variations are input in the model a priori and represent the effective viscosity in the given depth.

Results: First, we run the finite-element model till relaxation slows significantly, and then we continue the calculations by semi-analytical solution.

The evolution of the topographic relief for a model with 80-km thick crust and 1600 K mantle temperature is shown in Fig. 1. The relaxation is focused into a few hundred km thick belt along the dichotomy boundary. After 30 years the topography changes by 1 km. The plastic strain develops in four locations: 1) 200-300 km south of the dichotomy boundary (tension), 2) 200-300 km north of the boundary (compression), 3) along the bottom of the slope of the boundary (tension) and 4) along the top slope (compression). The model with 35-km thick crust and 1600 K mantle temperature behaves similarly, only relaxation occurs more slowly.

Our semi-analytical solutions match the finite-element solutions assuming a simple two-layered

constant-viscosity profile. Continuation of the finite-element calculations by semi-analytical modeling shows that 80-km thick crust relaxes too fast to preserve the long topographic wavelengths over 3 Gyr, even if cooling of the Martian interior is considered. If we assume plausible cooling rates, the 35-km thick crust will allow the preservation of long wavelengths while relaxing the 300-500 km wavelengths.

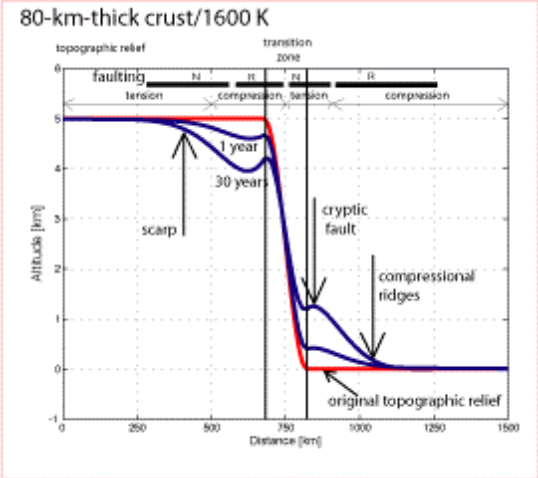

Fig. 1: Topographic relaxation, plastic strain (faulting), and stress distribution on surface of the finite-element model.

In order to preserve the long topographic features (10,000 km) over 3 Gyr and relax the 300-500 km wavelengths within 0.5 Gyr, the contrast of effective viscosity between the upper and lower crust must be 4-6 orders and a lower crustal channel of 10 km thickness must develop. The viscosity of the lower crust of 10^19 Pa s for 35-km thick crust, or 10^21 Pa s for 80-km thick crust, averaged over 30 Myr, (Fig. 2) provides a reasonable viscosity estimate that satisfies both criteria. The viscosity is one order higher if we average over 300 Myr time. If cooling rates are taken into account, lower viscosities will be allowed.

Conclusion: Our finite-element model predicts relaxation of the topography within several hundreds km along the dichotomy boundary. The relaxation, and the faulting associated with the relaxation, matches the geologic observations in the Ismenius region. The faulting, located 200-300 km south from top slope of the boundary, probably results in a steep scarp. Thus relaxation of a gently sloped boundary, as predicted by many formation models [14] can result in the steep slopes observed in many areas today. The deformation of the boundary is dependent on the lower crustal rheology, which is dependent on the crustal thickness and temperature. From our finite-element modeling, the temperature gradients of 20 K/km 4 Gyr ago provides the best fit to the geologic observations. This gradient is consistent with those inferred from elastic thickness estimates [15].

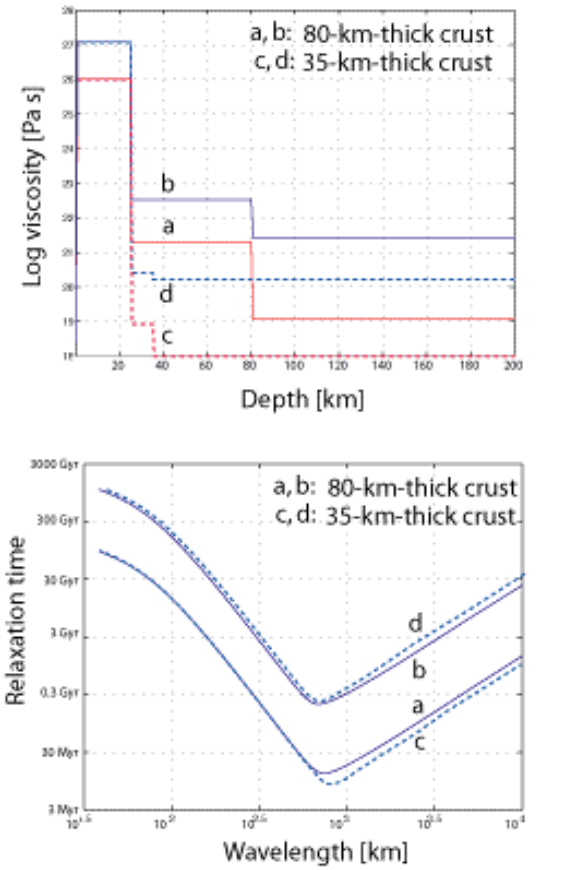

Fig. 2: The viscosity profiles (top) and relaxation curves (bottom) that will preserve 10,000 km features over 3 Gyr and relax 300-500 km features in 0.5 Gyr. Curves a and c average viscosity over time 30 Myr, curves b and d average viscosity over 300 Myr.

References: [1] McGill G. E. and Dimitriou A. M. (1991) JGR, 95, 12595-12605. [2] Frey H. V. (2004) LPSC XXXIV, #1382 [3] Frey H. A. et al. (1998) GRL, 25, 4409-4412. [4] Smith D. E. et al. (1999) Science, 284, 1495-1503. [5] Zuber M. T. et al. (2000) Science, 287, 1788-1793. [6] Frey and Schulz, (1988) GRL, 15, 229-232. [7] McGill et al., 2004, this volume [8] Smrekar S. E. et al. (2004) submitted to JGR. [9] Nimmo F. and Stevenson D. J. (2001) JGR, 106, 5085-5098. [10] Mackwell, S. J. et al. (1998) JGR, 103, 975-984. [11] Nunes D. and Phillips R. (2004) JGR, 109, E01006 [12] Chopra P. N. and Paterson M. S. (1984) JGR, 89, 7861-7876. [13] Cathles, L. M. (1975) The Viscosity of the Earth's Mantle, Princeton University Press, [14] Zhong S. and Zuber M. T. (2001) EPSL, 189, 75-84 [15] McGovern et al. (2003) JGR, 107, 5136.

APPLICATION OF RECENT MISSION RESULTS TO THE ORIGIN AND EVOLUTION OF THE DICHOTOMY BOUNDARY. J. W. Head, Dept. of Geol. Sci., Brown Univ., Providence, RI 02912 USA, james_head@brown.edu.

Introduction and Background: The origin of the dichotomy boundary and the processes that have been responsible for its modification since its formation have been a matter of debate and speculation ever since the distinctive contrast the northern lowlands and cratered southern uplands was first discovered. Part of the difficulty in making significant advances on these problems has been the lack of new data. The recent focus on the exploration of Mars has considerably changed this and the prospect of even more new data promises to bring major advances in the characterization of the crust of this region and new insight into its origin and evolution. The purpose of this contribution is to review some of these new data and to point out where new advances are likely to be made.

Geophysical data: The Mars Global Surveyor (MGS) mission acquired abundant new geophysical data, including improved gravity, topography, and magnetic field data (Fig. 1, radial magnetic measurements on MOLA shaded relief). These data have permitted new determinations of crustal thickness, and the relative types and intensity of magnetic anomalies in the northern lowlands and southern uplands and across the boundary (Fig. 1). Radar instruments such as MARSIS on Mars Express and SHARAD on MRO are designed to probe and to profile the subsurface to add to the three-dimensional view of the shallow crust and differences across the dichotomy boundary.

Crustal mineralogy and chemistry: Interpretations of crustal mineralogy and chemistry have been forthcoming from the thermal emission spectrometer (TES) on MGS and THEMIS and the GRS/NS complement of instruments on Mars Odyssey. Furthermore, surface exploration and rock and soil analyses by the Mars Exploration Rovers have provided ground truth for surface geological units. The Mars Express OMEGA spectrometer and the multispectral High Resolution Stereo Camera (HRSC) together provide high spatial and spectral resolution data at wavelengths complementing previous missions. Upcoming Mars Reconnaissance Orbiter mission experiments, such as CRISM, will also contribute both high spatial and high spectral resolution data.

Surface physical properties: TES and THEMIS data have opened up a whole new world of interpretation of the physical properties of surface units such as slopes and crater ejecta deposits. Quantitative thermal inertia data have been useful in understanding the distribution of rocks and soils on the surface and the relative ages of some units.

Geological data: The dichotomy boundary is known to have undergone significant modification since its formation and the nature of this modification provides information on the processes responsible for the destruction and lateral migration of the boundary, as well as clues to its original configuration. The acquisition with MGS of very high-resolution images (MOC) and global altimetry (MOLA), combined with the improved spatial resolution and spectral diversity of THEMIS images, has revolutionized the analysis of these processes.

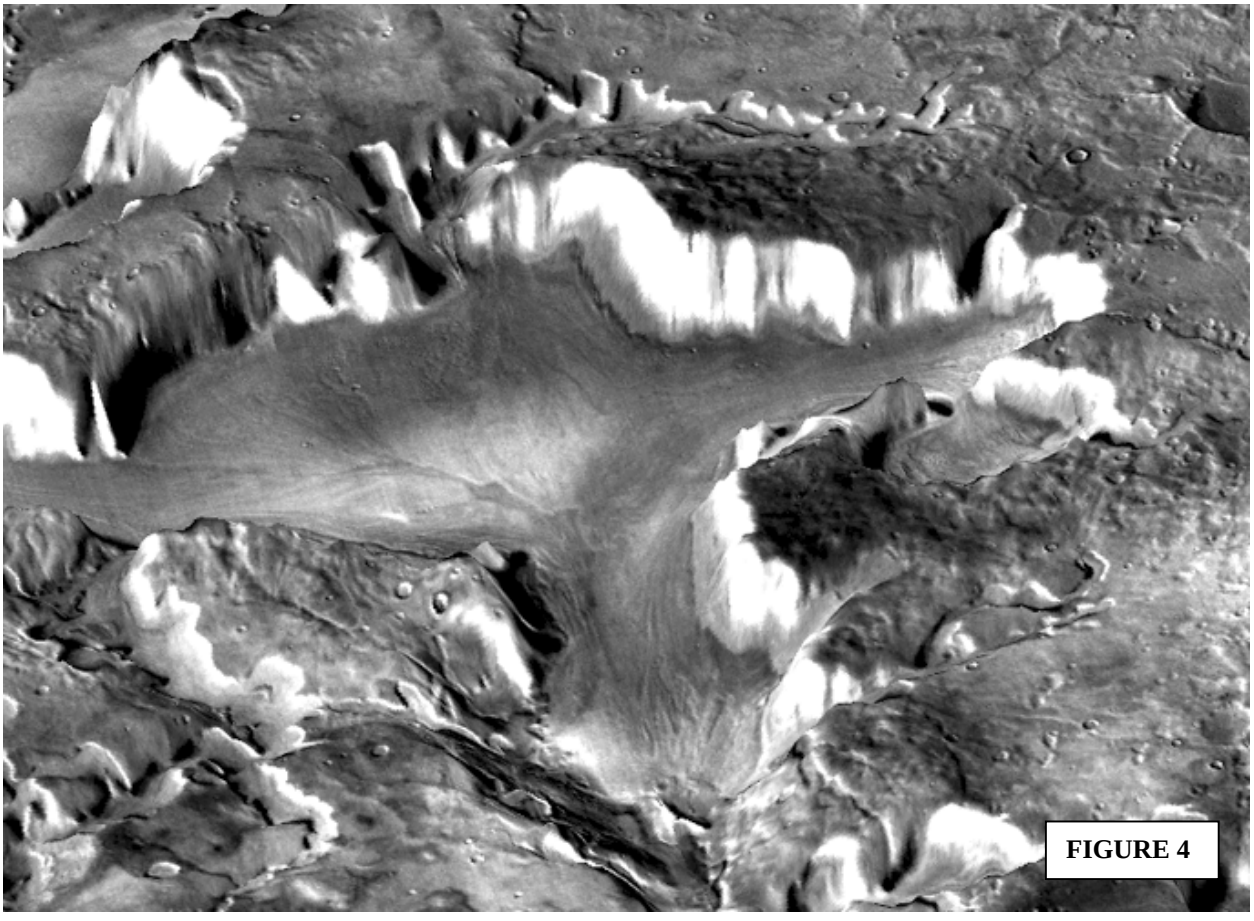

FIGURE 4

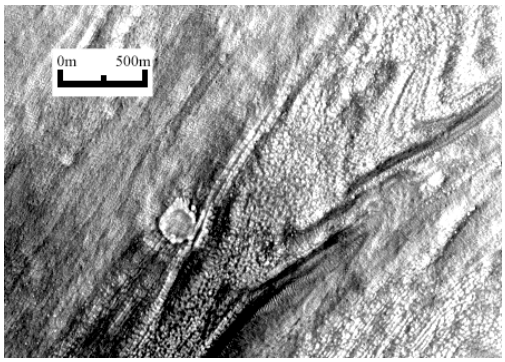

FIGURE 5C

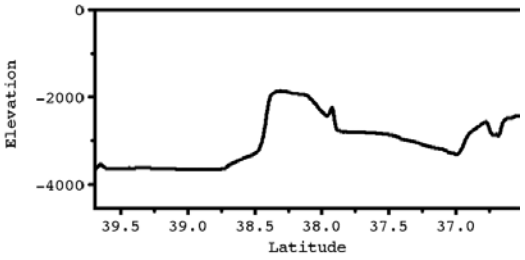

FIGURE 3

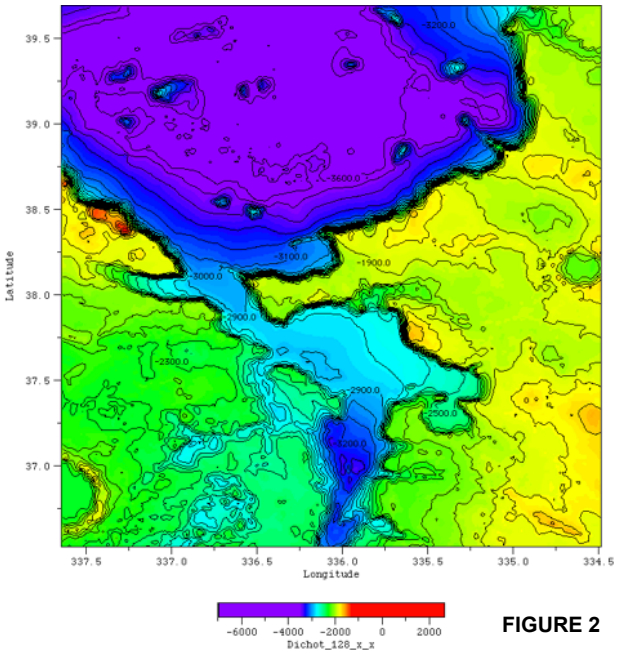

FIGURE 2

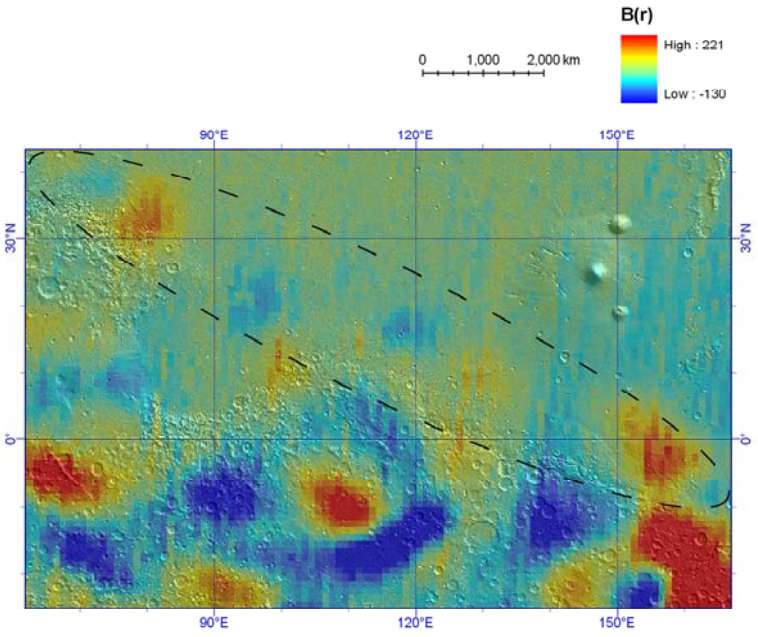

FIGURE 1

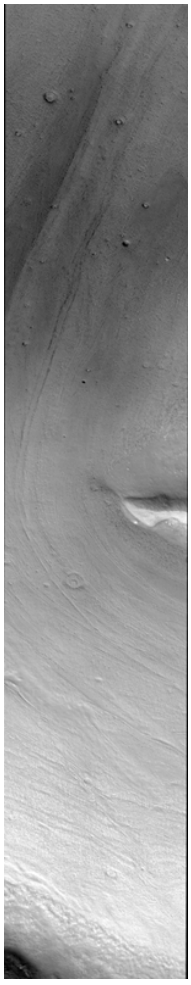

FIGURE 5A

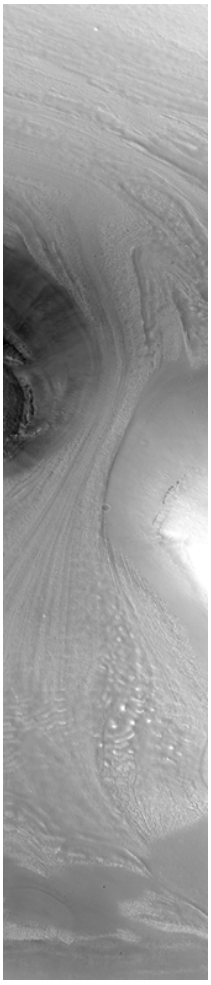

FIGURE 5B

For example, it is now possible to compile detailed high-resolution topographic maps of Mars (Fig. 2) that can combine contours, color-coded topography and shaded relief. Altimetric profiles (both directly from individual data swaths and from the gridded data; Fig. 3) provide abundant information about landform morphometry and slopes. THEMIS images can be draped over the topography data to visualize geological relationships and assess unit characteristics (Figure 4). Very high-resolution MOC images reveal spectacular detail (Figure 5a, b, c) and provide new insight into the nature of processes modifying the dichotomy boundary. Data to be obtained by the HiRISE imaging experiment on the upcoming MRO mission will be of even higher resolution.

These new data, for example, have revealed evidence for the accumulation and flow of ice in glacial-like patterns in and near the dichotomy boundary (e.g., Figures 1-6).

MARS DICHOTOMY BOUNDARY DEGRADATIONAL PROCESSES: EVIDENCE FOR EXTENSIVE AMAZONIAN GLACIATION. J. W. Head[1], M. C. Agnew[1], C. I. Fassett[1], D. R. Marchant[2] and M. A. Kreslavsky[1] [1]Dept. of Geol. Sci., Brown Univ., Prov., RI, 02912. [2]Dept. of Earth Sciences, Boston Univ., Boston, MA 02215.

Among the hallmark morphologies of the dichotomy boundary, particularly at higher latitudes are 1) the debris aprons the surround many of the massifs and valley walls, and 2) the lineated valley fill that occurs in many of the valleys themselves (1-11). The ages of these deposits are typically much younger than the adjacent plateau terrain or its breakup and the formation of the valleys themselves (e.g., 8, 11). The margins of the debris aprons are rounded and convex upward topography, and the debris aprons and the valley fill can appear smooth and relatively homogeneous or, in contrast, can be characterized by closely spaced parallel ridges and grooves a few to several tens of meters high. These sets of parallel ridges have been interpreted to have formed both parallel and normal to valley and mesa walls. Some (1) argue that the lineations for mostly normal to flow due to converging flow from debris aprons on opposite sides of valleys or mesas, while others (3) argue that bending of ridges and grooves entering valleys from a side tributary supports flow in the direction parallel to the valley. All agree that the materials represent some sort of viscous flow processes, but opinions differ on the details of the mechanism; most authors call on processes of gravity-driven debris flow, assisted by ice or water in the interstices derived from either groundwater or the atmosphere (e.g., see 6, 9-11).

New THEMIS, MOLA and MOC data provide additional perspectives on the origin of the debris aprons and lineated valley fill, suggesting that at least in some areas, glaciation (accumulation of snow and ice to sufficient thickness to cause its local and regional flow) may have played a significant role. We have analyzed numerous areas along the dichotomy boundary north of 30 degrees north latitude and present the results from one area as an example. In this region (Fig. 1) just south of Deuteronilus Mensae, a T-shaped valley occurs just south of a large depression. The walls of the large depression are characterized by debris aprons and there is a break in the southern rim of the depression that leads to the top of the T-shaped valley (about 100 km across). A topographic profile (Fig. 2) from the floor of the large depression across the southern wall, across the top of the T and along the vertical part of the T shows 1) the flat floor of the large depression, 2) the classic convex upward slope of the debris apron, 3) the elevated floor of the top of the T, 4) the convex upward slope of the vertical part of the T. Note that the floor of the T-shaped valley along the top of the T lies at elevations as high as -2600 m, almost a kilometer above the large depression floor. Note too, that the bottom of the valley along the vertical part of the T is almost at the same level as the floor of the large depression. THEMIS data superposed on MOC altimetry and viewed perspectively shows strong evidence for flow lineations (Fig. 3), their characteristics and their directions; details of the lineations are shown in the MOC images (Figs. 4-6). Examination of Figs. 1 and 3 shows evidence of numerous lineations in the 20 km diameter crater south of the eastern arm of the T. The lineations on the floor of the crater converge and can be traced through the gap in the crater wall (Fig. 5, lower part) joining lineations beginning at the eastern edge of T (Fig. 5, upper right). Similar lineated valley fill extends from the mouth of a north-trending valley in the lower western part of the T, is deformed by valley lineations from valley fill apparently moving from the higher terrain to the west, and then joins the general lineated valley fill just to the east (Fig. 5). Furthermore, additional lineated valley fill begins at the base of the broad amphitheater on the western part of the top of the T, and converges with at the T-junction with the lineated valley fill coming from the west (Fig. 4) and the east (Fig. 5). From here, these three major flow lineation directions converge and extend down the vertical part of the T, with many of the lineations contorted at the margins of the convergence (Fig. 6). At the end of the major lobe, the topography is broadly convex upward (Figs. 2, 3) and the perspective view (Fig. 3) shows the distinctive lobe like nature of the lobe as it extends into the adjacent low-lying terrain.

What processes are responsible for the valley fill? These lineations and their complex patterns resemble flow lines in glacial ice, particularly where glacial ice converges from different directions at different velocities and deforms (compare Figs. 4, 6 and 7). Detailed analysis of the MOC, THEMIS and MOLA data suggests that changing environments and local topographic conditions (such as the crater wall and the narrow valleys) favored accumulation and preservation of snow and ice, and its glacial-like flow down into surrounding areas for distances approaching 70 km. Such environments are typical of snow and ice accumulation and debris-covered glacial flow in the Antarctic Dry Valleys, a cold polar desert analogous to the environment on Mars. Alternative hypotheses focus predominantly on groundwater or ice from atmospheric water vapor lubrication of debris flows (e.g., see 6, 9-11). We believe that the thickness of the deposit, the great lateral extent and continuity of flow lineations, and their complex interactions consistent with glacial-like flow, are all evidence that supports glacial-like flow of debris rich ice, rather than ice-containing debris. The relationship between the lineated valley fill and the classic debris aprons is not yet firmly established; however, the contiguous nature of many examples of lineated valley fill and debris aprons (Fig. 1) suggests that if the glacial interpretation of the valley fill is supported by further observations, then glacial ice may play more of a role in the formation of debris aprons than previously suspected.

The age of the deposits in this region are Amazonian (~300 Ma, with some of the deposits as young as 10 Ma (11)), broadly similar in age to the tropical mountain glaciers of Tharsis Montes and Olympus Mons (14). This suggests that there may have been periods during the Amazonian when tropical and mid-latitude glaciation were extensive. Thus, glaciation may have played a significant role in evolution of the dichotomy boundary during the Amazonian; significant amounts of ice could remain today in these valleys beneath a protective cover of sublimation till.

References: [1] Squyres, S.W. (1978), *Icarus*, 34, 600. [2] Squyres, S.W. (1979), *JGR.*, 84, 8087. [3] Luchitta, B.K. (1984), *LPSC XIV*, abs. no. B409. [4] Kochel, R.C. & Peake, R.T. (1984)

LPSC XV, abs. C336. [5] Carr, M.H. (1995), *JGR*, 100, 7479. [6] Carr, M.H. (1996), *Water on Mars*. [7] Colaprete, A. & Jakosky, B.M. (1998), *JGR*, 103, 5897. [8] McGill, G.E. (2000), *JGR*, 105, 6945 [9] Mangold, N. & Allemand, (2001), *GRL*, 28, 407. [10] Mangold, N. et al. (2002), *PSS*, 50, 385. [11] Mangold, N. (2003), *JGR*, 108, doi: 10.1029/2002JE001885. [12] Benn, D.I. & Evans, D.J.A. (1998), *Glaciers and Glaciation*. [13] Marchant, D.R. & Head, J.W. (2004), *LPSC XXXV*, abs. no. 1405. [14] Head, J.W. & Marchant, D.R. (2003), *Geology*, 31, 641. [15] Head, J.W. et al. (2003), *Nature*, 426, 797. [16] Post, A. & Lachapelle, E.R. (2000), *Glacier Ice*.

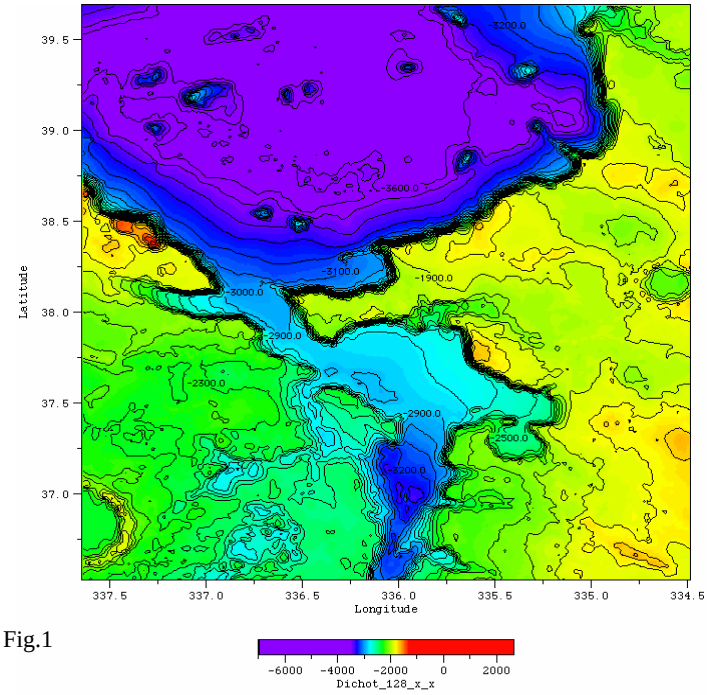

Fig.1

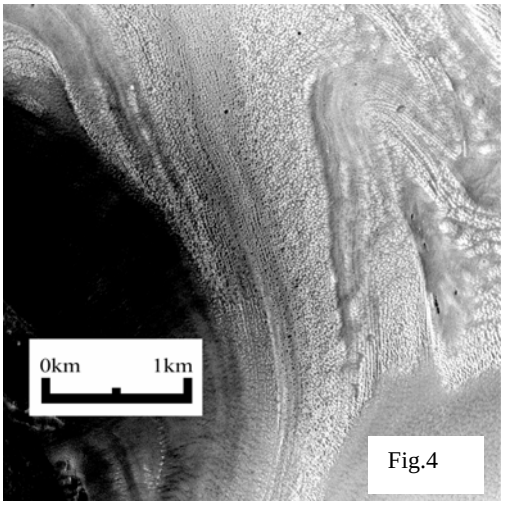

Fig.4

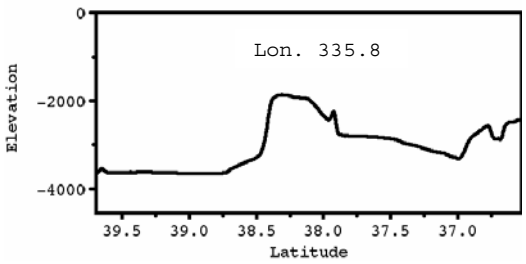

Fig.2

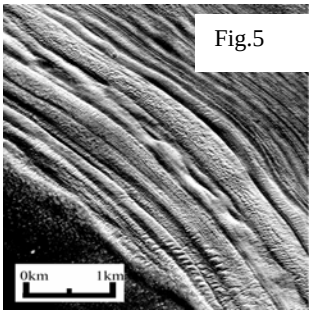

Fig.5

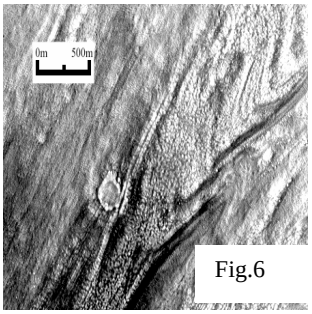

Fig.6

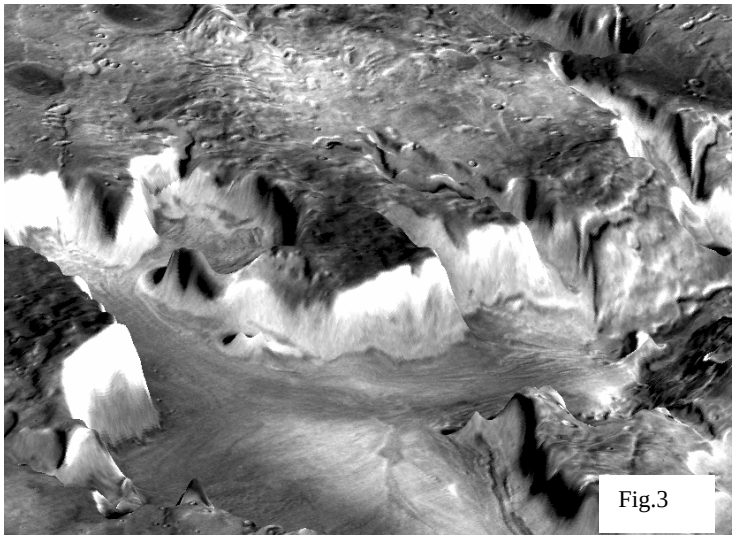

Fig.3

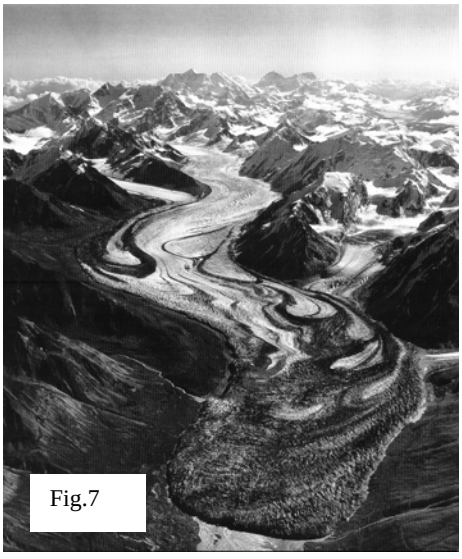

Fig.7

MARS DICHOTOMY BOUNDARY DEGRADATIONAL PROCESSES: MODEL OF THE NOACHIAN-HESPERIAN HYDROLOGICAL CYCLE. James W. Head[1], Michael H. Carr[2], Caleb I. Fassett[1], and Patrick S. Russell[1]. [1]Department of Geological Sciences, Brown University, Providence, RI 02912, [2]U. S. Geological Survey, 345 Middlefield Road, Menlo Park, CA 94025 (james_head@brown.edu)

Summary: The global climate of Mars is thought by many to have changed to its present cold and dry state from warmer and wetter conditions earlier in its history during the Noachian. Here we summarize evidence for a major transition in near-surface hydrogeologic conditions in the Late Noachian, and a fundamental change in the martian hydrological cycle. Hydrogeologic conditions then were characterized by five main domains: 1) an accumulation zone at higher altitudes, where atmospheric water entered the system through pluvial/nivial activity and was transported laterally by valley networks for tens to hundreds of kilometers before evaporating, sublimating, or completely reentering the vadose zone, 2) an upper mid-altitude region dominated by the vadose zone where pluvial/nivial activity was less important, and valley networks were much less common, 3) a lower mid-altitude region where the groundwater table occasionally reached the surface and theater-headed valleys and large fretted channels formed by groundwater sapping and headward retreat, 4) a lower altitude region, where the groundwater table normally (the dichotomy boundary) and where fretted and knobby terrain formed by large-scale groundwater sapping, and 5) a very low altitude region (the northern lowlands), largely below the groundwater table, where groundwater discharge accumulated. Variations in the exact altitude distribution of these zones and the often transitional boundaries between them, strongly suggest that the groundwater system was irregularly recharged during this period and that the groundwater table oscillated vertically with time. Changing atmospheric and near-surface conditions at the end of this period resulted in the freezing of the outer layers of the crust to form a global cryosphere. At the end of this period, the hydrological cycle changed from one which was vertically interconnected from the atmosphere through the surface and subsurface to the groundwater system, to a horizontally layered one in which the groundwater reservoir is separated from the surface reservoir by a global cryosphere, a condition that that still characterizes Mars today, ~3.5 billion years later.

Introduction and Background: Controversy surrounds that nature of early climatic conditions on Mars [1, 2]. In our approach, rather than trying to uniquely determine the nature of the Noachian climate from the geological record (e.g., valley networks [3]) or from global climate models [4], we have adopted the strategy of using the present environmental conditions (cold dry polar desert [5]) as a baseline, and working back in geological time until the geological evidence forces us to the conclusion that the climate must have been different. When and if such evidence emerged, this information might provide insight into the manner in which the environment changed and thus provide independent insight into Noachian climatic conditions. We outline elsewhere [6] the detailed evidence that leads us to the conclusion that cold, dry polar desert conditions and a globally continuous cryosphere [7] characterized the martian climate and near-surface conditions as far back as into the Early Hesperian. Local breaching of the cryosphere and outflow of sequestered groundwater characterized major hydrogeological activity during this 3+ billion year period, and although short-term climate variations may have occurred at these times [8], any changes appear to have been insufficient to alter the globally continuous cryosphere. Three major types of features common in the Late Noachian signal a fundamental change in these conditions: 1) **Fretted and knobby terrain**, which we interpret to represent the presence of a groundwater table intersecting the surface, and the consequent sapping and erosion of the globe-encircling highland-northern lowland boundary [9]. **2) Theater-headed valleys/Fretted channels/Large valley networks**, which we interpret to represent groundwater sapping occurring commonly near the dichotomy boundary, and focused sufficiently to cause significant erosion and headward retreat to form large sapping valleys [10]. 3) **Valley networks**, [e.g., 3, 11] which occur primarily at higher elevations [1] are interpreted to represent overland flow and seepage of water and channelization; we interpret these to represent the result of pluvial/nivial activity and to produce recharge through the vadose zone into the groundwater system [12]. Previously, we have outlined the basic hydrologic principles that govern the hydrological cycle and related processes in environments like those on Mars [13,14]. Here we outline a synthesis of these findings that describe a model of Late Noachian hydrogeology and the transition to a radically different hydrologic cycle than that in existence today [e.g., 7, 15].

The Late Noachian Hydrologic System: We believe that the Late Noachian hydrologic system shares many of the basic characteristics of the present terrestrial hydrologic cycle [13,14], modulated by some of the conditions described above. On the basis of our interpretation of the major terrain types listed above, we envision the hydrogeologic elements and hydrologic cycle at this time as follows.

The most critical element for recognizing the nature of the hydrological cycle is the location of the top of the groundwater system, the water table. This most commonly occurs in the subsurface in land areas on Earth, or at the edge of large standing bodies of water, such as lakes, seas and oceans, where the margins of the water body and the water body equipotential surface itself delineate the water table. On Mars, any Late Noachian standing body of water [e.g., 15] is no longer present, and thus indirect evidence must be sought as to its location.

We interpret the fretted and knobby terrain occurring at the dichotomy boundary and encircling the majority of the boundary between the northern lowlands and the southern uplands at elevations between -1 and -4 km to represent the approximate location of the water table during the Late Noachian [9]. The fretted and knobby terrain is clearly derived from the collapse and degradation into knobs and mesas of adjacent upland cratered terrain. On the basis of 1) its very widespread distribution around almost the entire edge of the exposed upland terrain at the northern lowland boundary, 2) its apparent Late Noachian age (although degradation processes continued to modify it), and 3) its consistent distribution in terms of altitude range [9], we interpret this unit as marking the location of the water table and having originated in the following manner. Above this general level, the surface of Mars was a zone of infiltration, where water falling on the surface ultimately percolated vertically through the vadose zone into the saturated zone and then flowed laterally. In the vicinity of the north-south dichotomy boundary scarp, the water table intersected the surface [7]. In this region, ground-

water flows through the porous rock and soil layers discharged to the surface by seepage, and by localized flow as springs. This eroded and undercut the surface topography causing channelization and backwasting of the scarp and upland cratered terrain. Discharged water and sediment flowed downslope into the northern lowlands. If this fretted and knobby zone is correctly interpreted as the location of the water table, then its presence means that groundwater readily exchanged with the surface on a global scale and that the global cryosphere had not yet developed. Furthermore, the fact that this terrain is not seen in any abundance in younger terrain elsewhere on Mars suggests that this extensive distribution is revealing geological processes that are not common later in Mars' history.

What were the processes responsible for charging and recharging the global aquifer under these conditions? The valley networks provide evidence for the presence of liquid water, surface runoff, and stream activity at higher elevations in the southern uplands. Their presence strongly suggests that water was falling onto the surface due to pluvial or nivial activity, leading to subsequent overland flow and stream channel formation. Valley networks are more common at higher elevations [16,17] in the southern uplands and occur on the flanks of craters at the highest elevations there. If the valley networks were to represent *effluent streams* drawing groundwater from the surrounding regions and were also undergoing significant related groundwater sapping, as envisioned by some [e.g., 16], then the implication is that the water table is just below the surface at elevations of ~3 km, for example in the circum-Hellas highlands. This implies that the global water inventory involves virtually all crustal pore space and thus provides a global water volume well in excess of 1 km global equivalent layer [1,7]. Instead, we believe that the upper part of the regolith in the highlands represents the vadose zone and that the water table occurs at a much deeper level below the surface. We interpret valley networks to be *influent streams*, not *effluent streams*. As *influent streams*, valley network channels form from collection of overland flow from pluvial or nivial water deposition on the surface, lateral transport in the channels, and ultimate drainage down into the vadose zone over the course of their flow. In this manner, they feed the groundwater system largely from above and maintain the level of the water table, which varies depending on the amount of water entering the groundwater system by precipitation and infiltration and the amount leaving the system, for example by evaporation or sublimation back into the atmosphere. Although the depth to the water table is not necessarily constant across the surface, the location of the intersection of the water table and the surface in the fretted and knobby terrain suggests that there may be as much as 3-4 km between the highest surface in the southern uplands and the water table there. This strongly suggests that there is a vadose zone in the southern uplands that may be up to several kilometers thick, depending on rates of infiltration and recharge.

Evidence supporting the presence of a vadose zone comes from the mid-altitude region of the southern uplands where valley networks are much less common. We interpret these to represent areas where pluvial/nivial activity was much less important than in the highlands, and where valley networks had largely lost their transported water by influent processes and seepage and infiltration into the vadose zone. In this model, the lower abundance of valley networks at lower elevations are a natural consequence of their formation in the vadose zone and their influent behavior. Indeed, the unusual nature of many aspects of valley networks [17] can be readily explained by influent streams. If this interpretation is correct, convolved in their characteristics is important information about soil porosity and permeability, and water flux [12].

Located in a zone between the fretted/knobby terrain and the valley networks is a series of very large valley network-like features known as fretted channels and theater-headed valleys [17]. These are broad, flat-floored, steep-walled valleys up to 20 km wide that extend from the margins of the northern lowlands deep into the uplands. The presence of headward linear closed depressions and collapsed margins strongly suggest that the channels and valleys formed by subsurface groundwater movement and sapping [17]. They are primarily located between elevations of -3 km and +1 km, overlapping with the elevation range and area in which there are fewer valley networks. The range in the elevation distribution of the sapping channels may be due to their headward erosion, or could signal differences in the level of the water table. More discharge into the regolith would raise the water table and enhance sapping at higher levels. Alternatively, as the northern lowlands freeze and the cryosphere migrates southward, perhaps the water table rises and the groundwater builds up hydrostatic head [10].

Summary: These data and correlations, and the similarities to terrestrial hydrogeologic features and the hydrologic cycle, suggests that this model (Fig. 1) may reasonably approximate the nature of the Late Noachian hydrologic cycle. This scenario predicts that the northern lowlands were largely below the level of the water table and thus may have been flooded, although the high latitudes indicate that much of the region might have been frozen. This scenario and hydrologic system configuration optimizes the erosion and modification by significant seepages, fluvial activity, and sapping, all leading to erosion and retreat of the dichotomy boundary during the Noachian and Hesperian.

References: [1] Carr , M. H., *Water on Mars*, Oxford, 1996. [2] Pollack, J. et al., *Icarus*, 71, 203-224, 1987. [3] Craddock, R. and A. Howard, *JGR*, doi:10.1029/2001JE0011505, 2002. [4] Haberle, R. *JGR*, 103, 28467-28490, 1998. [5] Hecht, M., *Icarus*, 156, 373-386, 2002. [6] Head, J. and L. Wilson, LPSC 32, #1218, 2001. [7] Clifford, S., *JGR*, 98, 10973-11016, 1993. [8] Baker, V., *Nature*, 412, 228-236, 2001. [9] Head, J. et al., *Vernadsky-Brown Microsymposium 38*, ms30,31, 2003. [10] Head, J., et al., *Vernadsky-Brown Microsymposium 38*, ms28, 29, 2003. [11] Hynek. B. and R. Phillips, *Geology*, 29, 407-410, 2001. [12] Fassett, C. and J. Head, *Vernadsky-Brown Microsymposium 38*, ms16, 17, 2003. [13] Head, J. et al., *Vernadsky-Brown Microsymposium 38*, ms26, 2003. [14] Head, J. et al., *Vernadsky-Brown Microsymposium 38*, ms27, 2003. [15] Clifford, S. and T. Parker, *Icarus*, 154, 40-79, 2001. [16] Grant, J., Geology, 28, 223-226, 2000. [17] Carr, M. *JGR*, 100, 7479-7507, 1995.

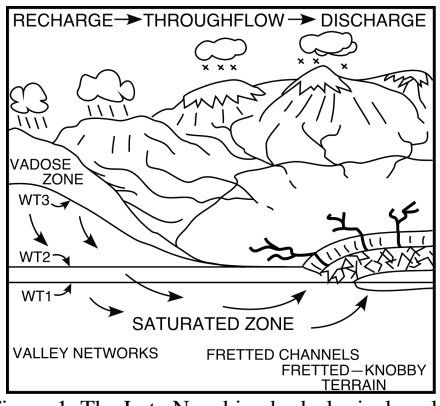

Figure 1. The Late Noachian hydrological cycle.

MARS DICHOTOMY BOUNDARY DEGRADATIONAL PROCESSES IN SPACE AND TIME: CLUES TO GLOBAL CLIMATE EVOLUTION. James W. Head and Caleb I. Fassett. Department of Geological Sciences, Brown University, Providence, RI 02912, (james_head@brown.edu)

Introduction

It has long been known that the boundary between the northern lowlands and the southern uplands (the dichotomy boundary) is characterized by both a generally distinctive topographic change, as well as characteristic geological units that appear to represent processes of weathering, topographic degradation and scarp retreat southward from the dichotomy boundary. We first examine the nature and distribution of the units that characterize this boundary and then discuss how modification processes have varied over time and space

General description and distribution. A variety of terrains characterize the dichotomy boundary (Figures 1-4). At the largest scale (1:15M; [1-3]), the southern uplands are characterized by a variety of Noachian-aged units, most prominently the Plateau and high plains assemblage [1,2] of units, of which the Plateau sequence is the most important. Members of the Plateau sequence form "rough, hilly, heavily cratered to relatively flat and smooth terrain, covering most of the highlands". The most widespread of the units there are of Noachian age and include the heavily cratered units (Npl1 and Npl2), the heavily cratered unit dissected by a higher density of valley networks (Npld), an etched terrain "similar to the cratered unit but deeply furrowed by sinuous, intersecting, curved to flat-bottomed grooves producing an etched or sculptured surface" (Nple), and smoother intercrater ridged plains of possible volcanic origin (Nplr). The surface of the northern lowlands, on the other hand, is largely covered by the younger Hesperian-aged Vastitas Borealis Formation, and older units are virtually absent at the surface [1-3].

The intervening area between the southern uplands and the northern lowlands, commonly referred to as the dichotomy boundary, is a broad region hundreds of km wide that extends along the border and has a variety of units with a range of ages. Previous mappers at the 1:15M scale have put a symbol on the map described as the "Highland-Lowland boundary scarp" which was defined as a "Diffuse zone of transition between highland and lowland physiographic provinces" [1-3] (Figs. 1-4). One of the most prominent units in association with this zone is mapped as HNu, Noachian-Hesperian, undivided [1,2]. This unit forms "closely spaced conical hills a few kilometers across whose distribution indicates that they are remnants of numerous craters." The unit also "forms rugged terrain on margins of cratered plateaus, and isolated remnants..." The unit is gradational with the Apk, the Amazonian-aged knobby plains material, where the two units adjoin, but hills in the HNu unit "are more closely spaced, larger, and occupy more that about 30 percent of the area." The HNu unit is interpreted as "eroded remnants of ancient cratered terrain produced by mass-wasting processes, possibly as result of removal of ground ice..." Etched plains material (AHpe) is composed of irregular mesas and pits, and ranges from mid-Hesperian to to mid-Amazonian in age [1-3]. Also characteristic of the boundary at this scale are outflow channels of Hesperian age and younger channels of Amazonian age, both of which strike generally normal to the slope of the dichotomy boundary and modify it.

Later regional units obscure and heavily modify large portions of the dichotomy boundary (the Tharsis volcanic complex, the Chryse basin and outflow channel complex, and the thick mantling deposits of the Medusae Fossae Formation). We now proceed to characterize the broad dichotomy boundary zone where it is not obscured by later events (Fig. 1).

Detailed Areal Distribution. One of the most prominent and aerially significant developments of this terrain occurs in the Deuteronilus Mensae region, extending ~1500 km from about 320 to 355 W, and occupying a band of terrain up to ~800 km wide along the northern lowland-southern upland dichotomy boundary. In this region, the terrain spans an elevation range from ~-4 km to ~-2 km. It is largely made up of fragmented and isolated islands of Hesperian ridge plains (Hr) and Noachian plains, where the fragments are large enough to map as specific outcrops, rather than components of a separate specific unit, as with HNu. Also mapped are large swaths of Apk, in the lows between the large islands, and preferentially toward the eastern edge of the region.

A second major area of development is adjacent to Deuteronilus, extending eastward along the dichotomy boundary for about 2400 km from ~275 to 320 W to the Isidis Basin. Here the terrain is more knobby and occupies a 500-700 km wide belt that spans an elevation range from ~-3 km to ~0 km. The major map unit in this area is HNu, with minor amounts of Apk.

East of the break in the dichotomy boundary formed by the Isidis Basin, the knobby terrain reappears in a swath at, and parallel to, the dichotomy boundary extending from the eastern rim of Isidis (~260 W) for about 4700 km to the vicinity of 180 W, before it becomes largely mantled by the younger Medusae Fossae Formation. In this region, the elevation range is about -2 km to 0 km. The major unit mapped in the eastern part of this area is HNu, with minor amounts of Apk. At the crater Gale (~222 W) the proportion changes so that to the east of Gale, Apk dominates.

Description of the dichotomy boundary using MOLA detrended topography: MOLA detrended topography (Fig. 4) where the regional slope has been removed and local slope variations are enhanced, is ideally suited to demonstrate the nature of the progressive disintegration of the southern uplands at the dichotomy boundary. Figure 4 shows a significant portion of this boundary between longitude 288W and 298W, and latitude 30 to 39N. At the base of the image, heavily cratered Noachian aged etched plains (Nple) [1,2] are exposed over the lower 200 km of the area. At the northern edge of this area, a series of complex generally east-west trending faults cut the Nple in to a series of polygonal blocks. Theater-headed valleys and channels form in and adjacent to these faults, and enlarge and often interconnect them. Northward of this, approximately in the middle of the image, is a broad, 150-200 km wide zone in which the polygonal terrain is further broken up and degraded into smaller polygons. This area is mapped as part of the Hesperian-Noachian undivided (HNu) terrain [1.2] and is clearly transitional to the larger blocks of polygons toward the southern uplands. In the upper right-hand part of the image, the terrain is mapped as Amazonian-Hesperian etched plains (AHpe) [1.2], characterized by irregular mesas and pits. This terrain is characterized by even smaller and more rounded knobs that appear to be transitional to the mesas and polygons of HNu. Thus, the case has been historically made that the units and facies that are mapped across the dichotomy boundary here represent the progressive degradation and mass wasting of the original margin of the dichotomy boundary (see summary in [3, 4]). The distance over which this terrain occurs suggests that the retreat in this area (Fig. 4) could have been 200-400 km.

Facies and terrains: In the broader context of this and related areas (Fig. 1-4) we observe a series of features and facies that characterize the dichotomy boundary across the zone. These features are not always all present in the same locations, and they also overlap with each other to some degree. They are as follows: **1) Unmodified plains/uplands terrain**: **2) Polygonized Craters (PCs):** These have polygons developed in crater interiors and often have exit channels, which are usually fretted valleys. **3) Theater-headed valleys (THVs):** These develop from PCs as well as the fracture zones and polygonal plateaus. **4) Fracture zones (FZs):** Linear fractures ranging from graben to valleys, that are narrow to wide and oriented usually parallel but sometimes normal to the

dichotomy boundary. **5) Polygonal plateaus (PPs):** These are highly polygonized plains units that have been cut by the fractures seen in the FZ, but along which erosion and removal of material has occurred. **6) Hummocky terrain (HT):** Transitional to polygonal plateaus; smaller and less distinct, more rounded, but has polygons interspersed throughout, with generally fewer toward the knobby terrain. **7) Knobby terrain (KT):** Abundant small knobs, smaller and lower elevation than the hummocks in the HT, occasional hummocks. **8) Etched terrain:** Appears to have undergone some combination of thermokarst and eolian reworking.

Summary and interpretation: On the basis of the successive degradation of the terrain as represented by the faulting, polygonization, polygon degradation to mesas, and their further degradation to knobs, and on the features mapped within the zone (theater headed valleys, sapping features, channels, etc.), we favor the interpretation that a significant amount of groundwater was involved in the initial degradation and subsequent retreat of the dichotomy boundary. We further hypothesize that this boundary represents the altitude region at which the water table intersected the surface in the late Noachian and into the early Hesperian. This boundary may thus be the focal point for the top of the groundwater system at this time. Above this existed the vadose zone in the southern uplands, and the water table sloped upward toward the southern uplands at an angle that was related to the level of recharge in the system at any given time.

Following this early period, geological evidence suggests that the cryosphere continued to thicken and to become regionally stable and then globally extensive and thick [e.g. 4]. During this transition period, groundwater leakage at the base of scarps may have continued and freezing water may have assisted the downslope movement of material to cause debris aprons and lineated valley fill [5; Fig. 4-16]. Additional evidence suggests that the lineated valley fill and perhaps many debris aprons were characterized by a significant percentage of ice, placing them beyond the realm of simple ground water or ground ice-assisted creep, and into the range of glacial and rock covered glacial activity. New MOC, MOLA and THEMIS data strongly suggest that many examples of lineated valley fill are the result of glaciation [e.g. 6]. We have mapped numerous examples of apparent glaciation and ice-assisted creep along the dichotomy boundary from Deuteronilus Mensae to near the Isidis Basin (about 30-50 degrees N). Between just NW of Isidis and Gale Crater (30N-10S), the dichotomy boundary is narrower and less complex, in part reflecting the lack of prominent debris aprons and lineated valley fill related to ground ice and glaciation in the mid-latitudes.

In summary, erosional processes operating on the dichotomy boundary have varied in time and space. Valley networks, groundwater flow and seepage, sapping, and channel formation all operated to modify the boundary in the Noachian and Hesperian. By the Amazonian, the presence of a global cryosphere had minimized the role of groundwater and the general cooling climate had enhanced the role of surface ice-assisted creep and possible glaciation. At this point, variation in orbital parameters cause insolation changes that from time to time made water ice stable in the 30-50 latitude region [e.g., 7] and 'ice ages' occurred. When these were of long duration, sufficient ice and snow could accumulate to make ice-assisted creep and glaciation a major process in the modification of the dichotomy boundary in the mid-latitudes [6].

Reference: [1] D. Scott and K. Tanaka, USGS Map I-1802A, 1986. [2] R. Greeley and J. Guest, USGS Map I-1802B, 1987. [3] K. Tanaka et al., JGR, 108, 8043, 2003. [4] S. Clifford, JGR, 98, 10973, 1993; S. Clifford and T. Parker, Icarus, 154, 40, 2001. [5] M. Carr, Water on Mars, Oxford, 229p., 1996. [6] J. Head et al, this volume. [7] J. Head et al., Nature, 426, 797, 2003.

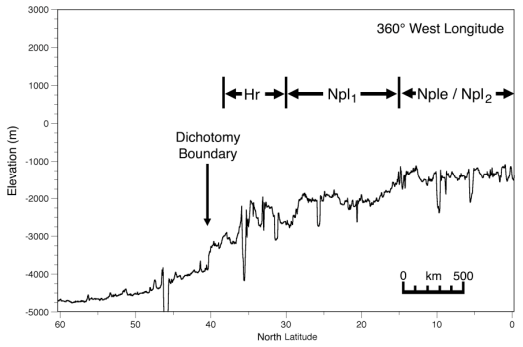

Figure 1.

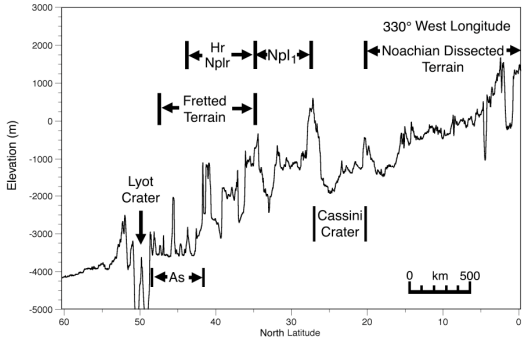

Figure 2.

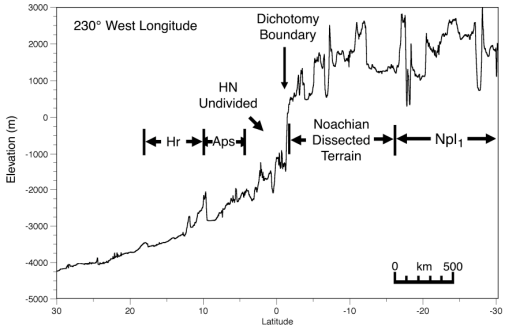

Figure 3.

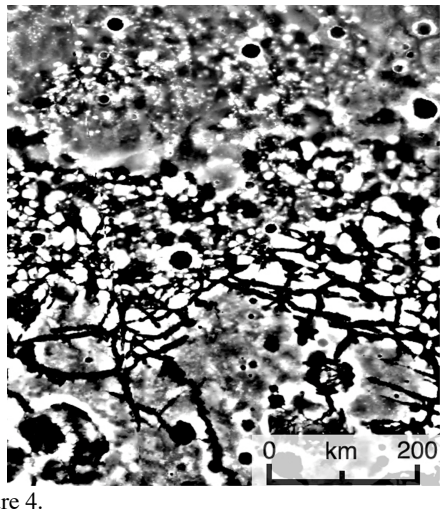

Figure 4.

CRUSTAL DICHOTOMY BOUNDARY AND FRETTED TERRAIN DEVELOPMENT AT AEOLIS MENSAE, MARS. R. P. Irwin III[1,2] and T. R. Watters[1], [1]Center for Earth and Planetary Studies, National Air and Space Museum, Smithsonian Institution, 4th St. and Independence Ave. SW, Washington DC 20013-7012, Irwinr@nasm.si.edu, twatters@nasm.si.edu. [2]Department of Environmental Sciences, University of Virginia, Charlottesville VA 22904.

Introduction: The origin of Martian fretted and knobby terrain has remained uncertain since the landforms were first described by Sharp in 1973 [1]. As a control on modeling efforts, it is important to establish the relationship of these landforms, if any, to the origin of the crustal dichotomy. Most studies have focused on fretted terrain in northern Arabia Terra, where investigators generally agree that ground ice has been important in modifying precursor knobs and fretted valleys [2–5]. The initial processes that isolated mesas from the high-standing terrain are less certain. Characteristics of some fretted valleys suggest an origin by fluvial erosion, despite their poorly developed drainage networks [5]. Other proposed mechanisms include crustal extension and structural control of sapping [6].

Situated near the martian equator at the crustal dichotomy boundary, Aeolis Mensae (Fig. 1) provides a pristine example of fretted terrain development without the younger landforms attributed to ground ice. We examined an area bounded by 15°S, 15°N, 120°E, and 150°E, adjacent to the cratered and dissected area described by Irwin and Howard [7]. Our observations indicate that Aeolis Mensae fretted terrain developed in a thick aeolian sedimentary deposit of late Noachian/early Hesperian age, which was emplaced along an older dichotomy boundary. Sediments were emplaced and eroded as fluvial activity declined, with minimal influence from highland valley networks.

Distinguishing highland bedrock from sedimentary deposits: The extensive degradation of Aeolis Mensae relative to the adjacent cratered highlands, where 20–50 m deep valley networks are preserved [7], suggests either that the mensae are composed of different materials than the highland crust, or that geomorphic proceses were concentrated along the dichotomy boundary [1]. Malin and Edgett [8] describe criteria for distinguishing sedimentary deposits on Mars from highland bedrock. Mesas in this area have boulder-free talus at MOC resolution, small-scale spur and gully morphology (suggestive of poorly cohesive materials, Fig. 2), massive and layered stratigraphic units, pedestal craters, knobs and yardangs, a near absence of fluvial valleys, and they overlie the termini of some valley networks in the area. The fretted materials supported high erosion rates on the order of 10^{-2} mm/year within fretted valleys, which formed only in materials with these morphologic characteristics. Fretted valleys breached crater rims in the plateau materials, but the rims are resistant to erosion when developed in the adjacent highland rocks. The fretted plateau deposits have thermal properties and rock abundances that suggest a well-sorted deposit of fine sand and smaller grains, which overlie coarser materials that are exposed at deflation pits and in ejecta [9].

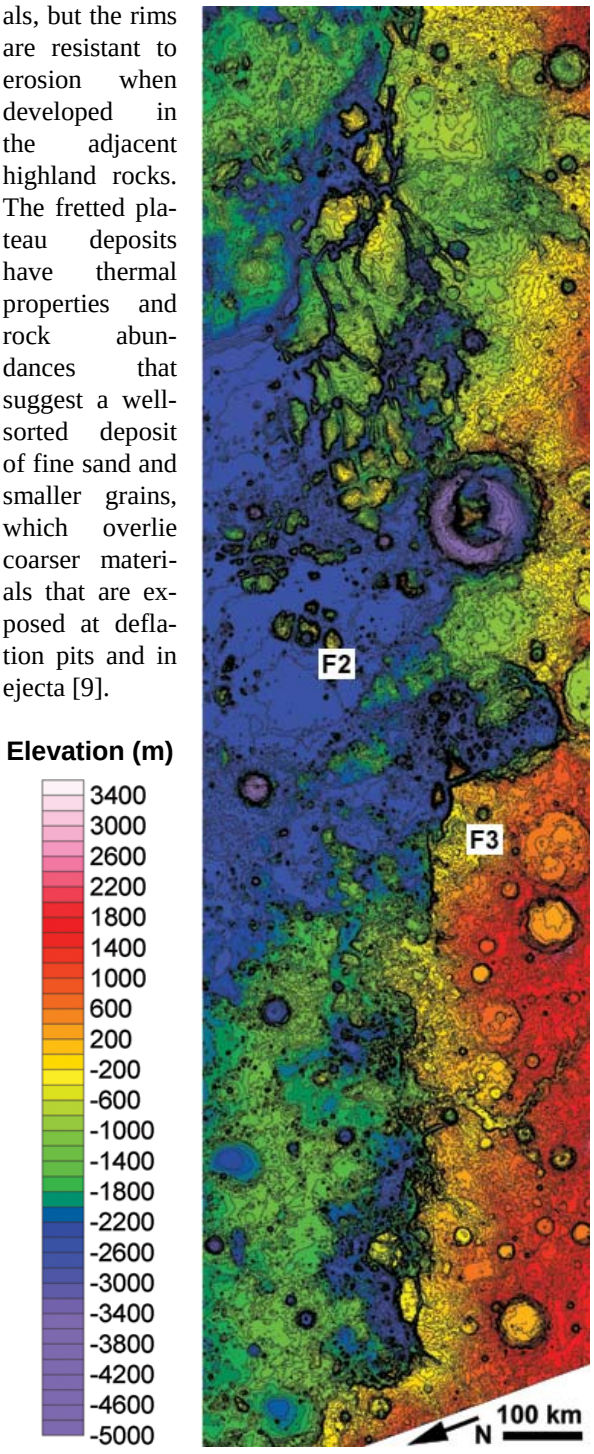

Fig. 1. Mars Orbiter Laser Altimeter topography of the study area in Aeolis Mensae, 1830 km across.

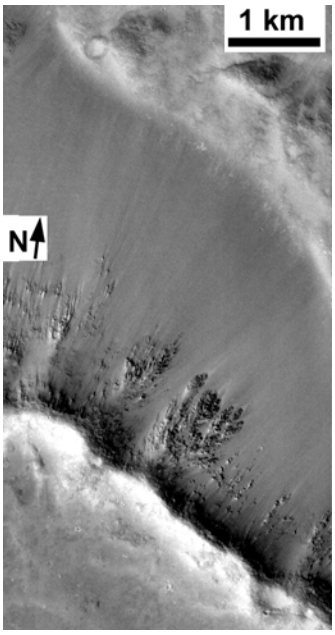

Fig. 2. Fluted valley crests and boulder-free talus on the an outlying isolated mesa in the fretted terrain. All observed outcrops in the fretted plateau materials have these characteristics, which suggest mass wasting of poorly cohesive materials without fluvial erosion. The strong albedo contrast at the base and crest of valley walls is an effect of high-pass filtering. MOC M10-03605.

Age relationships: Aeolis Mensae mesas and knobs are not dissected by valley networks as are adjacent highland slopes (Fig. 2). Most valley networks crossing the boundary have a hanging relationship with fretted valleys [7] (Fig. 3), consistent with a base-level reduction or southward advancement of the boundary scarp [7,10]. Fretted terrain likely formed between late Noachian/early Hesperian episodes of fluvial activity. These valley networks do not appear to continue into the lowland fretted/knobby terrains.

As a cratered slope underlies the fretted terrain, the dichotomy very likely predates the early Hesperian fretting processes [11,12]. Degraded crater morphology suggests that middle and late Noachian craters formed and were eroded on a precursor slope. Noachian craters are not modified by extensional faulting along the boundary in this area, as would be expected for a middle Noachian or later origin of the dichotomy. It is possible that a precursor dichotomy boundary slope dates to the early Noachian epoch (~3.95–4.5 Ga) and is coeval with the formation of the lowlands.

Possible emplacement and erosional processes: Observed aeolian deflation sites and pedestal craters require that the sediments were very well sorted, with no major lag-forming component of granules (2–4 mm) or larger particles. Whereas wind is a capable mechanism for sorting these particles, valley networks would probably deliver some coarse materials that would form a lag during deflation. Given few examples of fluvial valleys interacting with the fretted plateau deposit, it appears to have been emplaced mainly by wind. The confinement of the well-sorted deposit as a discrete sedimentary wedge along the older dichotomy boundary suggests emplacement primarily by aeolian processes from lowland sediment sources.

Erosion of these knobs may have been limited by the backwasting or disaggregation of the capping unit. Yardangs, etched terrain, absence of continuous flow paths, and the temporal relationships with valley networks favor wind as the main erosional medium [13].

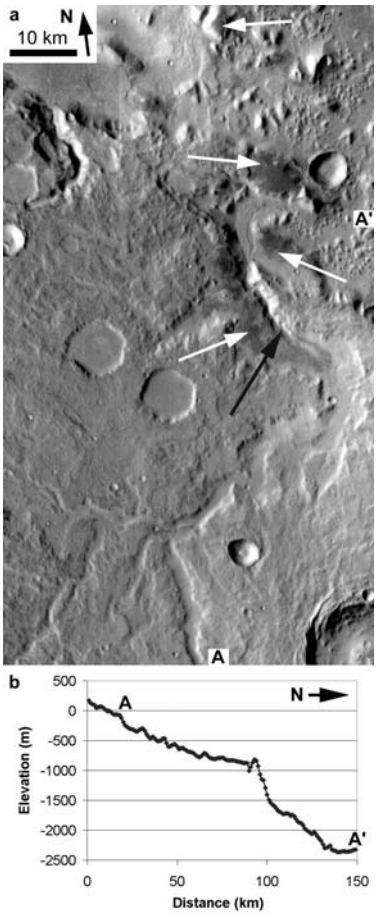

Fig. 3. Valley networks crossing the dichotomy boundary scarp. (a) A valley developed a wide floor with a –900 m base level, which is presently armored by relatively coarse materials (thermally dark in daytime IR, white arrows). Development of knobby terrain to the north caused a base-level decline to –2300 m and development of a knickpoint in the longitudinal profile (black arrow). Mosaic of THEMIS I02367004, I02005008, and I01306006. (b) Longitudinal profile of the valley in (a).

References: [1] Sharp R. P. (1973) *JGR*, 78, 4073–4083. [2] Squyres S. W. (1978) *Icarus*, 34, 600–613. [3] Lucchita B. K. (1984) *JGR*, 89, B409–B418. [4] McGill G. E. (2000) *JGR*, 105, 6945-6959. [5] Carr M. H. (2001) *JGR*, 106, 23,751–23,593. [6] McGill G. E. and Dimitriou A. M. (1990) JGR, 95,12,595–12,605, 1990. [7] Irwin R. P. and Howard A. D. (2002) *JGR*, 10.1029/2001JE001818. [8] Malin M. C. and Edgett K. S. (2000) *Science*, 290, 1927-1937. [9] Irwin R. P. et al., *JGR*, in press. [10] Kochel R. C. and Peake R. T. (1984) *JGR*, 89, C336–C350. [11] Frey, H. V. et al. (1988) *Proc. LPSC 18*, 679–699. [12] Maxwell T. A. and McGill G. E. (1988) *Proc. LPSC 18*, 701–711.

Gravity Modeling of the Isidis/Syrtis Major Region of Mars: Implications for Lithospheric Properties and for the Origin and Evolution of the Dichotomy Boundary

Walter S. Kiefer (Lunar and Planetary Institute, 3600 Bay Area Blvd., Houston TX 77058, kiefer@lpi.usra.edu, (281) 486-2110 (Office), (281) 486-2162 (Fax))

Introduction

Analysis of the gravity [1,2] and topography [3] of Mars provides our best view of the internal structure of Mars [4-9]. In this work, I model the gravity of the martian hemispheric dichotomy boundary in the region near the Isidis impact basin and Syrtis Major. I focus on two tasks. First, I estimate how the lithosphere's elastic thickness varies with location in this region of the dichotomy boundary. This constrains the thermal structure at the time the bulk of the topography was emplaced, roughly the first few hundred million years of martian history. Second, I develop models for the mascon beneath Isidis. The long-term preservation of this mascon constrains the thermal structure at the time of basin formation. Taken together, these results constrain the early thermal history of this portion of the dichotomy boundary. I use gravity model JGM95I-01, obtained from the Planetary Data System [10]. Results presented here are for spherical harmonic degrees 2 to 60, because the amplitude of terms above degree 60 are restricted by imposition of a power-law constraint in the gravity inversion.

Flexure Model

The thickness of the elastic lithosphere is an important parameter because it helps to constraint the thermal structure of the lithosphere at the time a topographic load was emplaced. The usual practice in planetary geophysics is to constrain the lithospheric thickness using a spectral admittance model [5-7]. However, this approach does not work well when substantial, uncorrelated surface and subsurface loads are both present in a region. In the Isidis/Syrtis region, there is 5.5 km of surface relief, and both the Syrtis Major cumulate chamber [8] and the Isidis mascon [1,2] are large subsurface loads, which limits the utility of the admittance approach.

As an alternative, I have assessed the lithospheric thickness by calculating the RMS misfit in the spatial domain between the observed gravity and a suite of models calculated assuming that the gravity anomalies are due solely to flexurally-supported topography [11]. The parameters that are varied in these models are the lithospheric thickness and the density of the crust. The mean crustal thickness is 50 km [9] and the mantle density is 3400 kg m^{-3} [12]. The elastic constants are appropriate for basalt.

The results in Figure 1 are for the region between 15° South and 0° North latitude and between 75° and 105° East longitude. For a crustal density of 2800 kg m^{-3} (intact, non-vesicular basalt), the best fit for the elastic lithosphere thickness is 10-15 km. The density of the crust could be reduced due either to vesicles in the basalt or by impact brecciation. Reducing the density to 2600 kg m^{-3} increases the required lithosphere thickness to 20-25 km. The minimum RMS misfit is virtually the same for the two density models and provides no means for distinguishing among them.

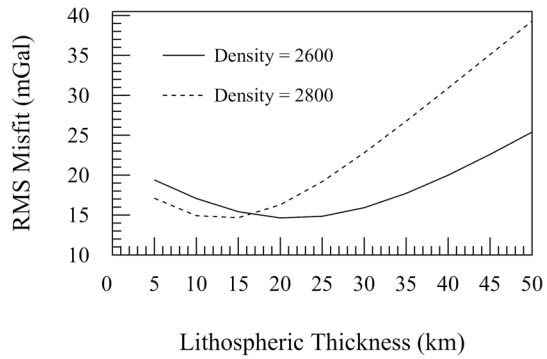

Figure 1: RMS gravity misfit as a function of elastic lithosphere thickness for the region south of Isidis. The solid line is for a crustal density of 2600 kg m^{-3}. The dashed line is for a crustal density of 2800 kg m^{-3}.

Other recent studies of the dichotomy boundary have favored relatively small crustal densities and a wide range of elastic thicknesses. Nimmo examined the dichotomy east of Isidis [7] and found a preferred elastic thickness of 61 km and a crustal density of 2500 kg m^{-3}. Kiefer [8] examined Syrtis Major, slightly northwest of the region studied here, and favored an elastic thickness of 5-15 km and a crustal density of 2600 kg m^{-3}. Preliminary modeling of the northwest part of the Isidis rim (20^0-40^o North, 50^o-80^o East) suggests that the lithosphere may exceed 30 km, but further modeling is required to assess the trade-off among model parameters and the possible role of bottom loading in that region.

Mascon Model

Isidis is one of the most prominent mascon basins on Mars. The peak gravity anomaly exceeds that expected from the surface topography by 440 mGal, requiring a substantial superisostatic uplift of the crust-mantle interface. Previous models have suggested that the mantle may reach within 3 km of the surface [4], assuming that the crust is relatively dense (2900 kg m^{-3}). If the crust is less dense due to impact brecciation or vesicularity, less mantle uplift is required. I am assessing these tradeoffs using a buried cylinder modeling method [8].

Regardless of the precise crustal density, it is clear that significant mantle uplift is required by the gravity data. Assuming that Isidis is similar in age to large lunar impact basins, this mantle uplift has been preserved against viscous relaxation for roughly 3.8 billion years. As a simple, first order approximation, this probably requires that the base of the elastic lithosphere was below the depth of the isostatic crustal thickness, roughly 50 km in this region, at the time of the Isidis impact. This result, combined with the elastic thickness results in Figure 1, indicates that the lithosphere in this region of Mars cooled and thickened rapidly in the first 700 Ma of martian history.

References

[1] Lemoine et al., *J. Geophys. Res.* 106, 23,359-23,376, 2001. [2] Yuan et al., *J. Geophys. Res.* 106, 23,377-23,401, 2001. [3] Smith et al., *J. Geophys. Res.* 106, 23,689-23,722, 2001. [4] Zuber et al., *Science* 287, 1788-1793, 2000. [5] McGovern et al., *J. Geophys. Res.* 107 (E12), doi:10.1029/2002JE001854, 2002. [6] McKenzie et al., *Earth Planet. Sci. Lett.* 195, 1-16, 2002. [7] Nimmo, *J. Geophys. Res.* 107 (E11), doi:10.1029/2000JE001488, 2002. [8] Kiefer, *Earth Planet. Sci. Lett.* 222, 349-361, 2004. [9] Wieczorek and Zuber, *J. Geophys. Res.* 109 (E01009), doi:10.1029/2003JE002153, 2004. [10] Mars Global Surveyor Radio Science archive volume mors_1024, Planetary Data System Geosciences node, http://pds-geosciences.wustl.edu, 2004. [11] Turcotte et al., *J. Geophys. Res.* 86, 3951-3959, 1981. [12] Bertka and Fei, *Earth Planet. Sci. Lett.* 157, 79-88, 1997.

The Crustal Dichotomy as a Trigger for Edge Driven Convection: A Possible Mechanism for Tharsis Rise Volcanism? S. D. King[1] and H. L. Redmond[2], [1&2]Department of Earth and Atmospheric Sciences, 550 Stadium Mall Drive, Purdue University, West Lafayette, IN 47907-2051, [1]sking@purdue.edu, [2]redmondh@purdue.edu

Introduction: A vertical constant temperature boundary is convectively unstable and drives convective motion. This is the essence of the Edge Driven Convection (EDC) hypothesis [1]. On Earth, cratonic keels [1] and continent-ocean boundaries [2] are locations where small-scale convection could be triggered from the vertical step in the thermo-chemical boundary layer at the surface. Because Earth has global, plate-scale motion, it isn't clear whether EDC instabilities can form at all (or any?) passive margins or cratonic keels; although seismic evidence supporting EDC has been observed under the African cratons [3].

While a mantle plume has been argued as the source of the volcanism that formed Tharsis rise, there are concerns that the plume model may not be consistent with other observations (e.g., thermal history calculations [5], the fact that there is a single large volcanic swell on the planet [6], and the ability to explain present day topography and gravity with crustal variations alone [7]). While none of these observations are strong enough to completely rule out a plume origin for the formation of Tharsis, the spatial correlation of the crustal dichotomy boundary and Tharsis rise is intriguing and a relationship between these has been suggested by a number of investigators.

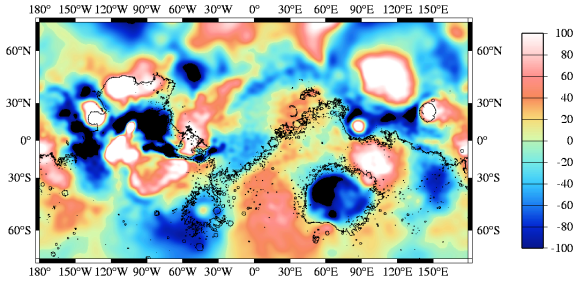

Figure 1. Spherical harmonic degrees 5-60 of the areoid. The black line is the zero contour of the topography, a proxy for the crustal dichotomy. There is no obvious correlation between the areoid and the elevation difference.

Mars is in a stagnant-lid mode of convection and inhibiting EDC by a plate-scale flow may not be a concern for Mars. Because of the lack of correlation between the areoid and the dichotomy boundary (Figure 1), it is almost certain that the crustal dichotomy has a vertical step much like passive margins or cratonic keels on Earth [4]. The question is whether this step is large enough to initiate a small-scale instability and whether this small-scale instability will survive long enough to produce the extended period of volcanism needed to create Tharsis rise.

Boundary Instability Questions: *1) Could the dichotomy boundary support a small-scale convective instability?* The answer to this depends on the differential crustal thickness and the gradient of the transition in crustal thickness between the northern and southern hemispheres. If we assume a crustal density of 2900-3000 kg/m^3, a mantle density of 3300-3500 kg/m^3, and an average dichotomy height of 4 km, an isostatic balance predicts a differential crustal thickness of 20-40 km. This alone seems to be insufficient to nucleate a small-scale instability. If the process that formed the southern hemisphere led to the development of a deep depleted layer beneath the southern hemisphere, much like cratonic keels on Earth, then the difference in 'crustal' thickness between the northern and southern hemispheres could be much larger than indicated by the simple isostatic balance and it might be reasonable to expect small-scale instabilities to form.

One additional complication is that maintaining stable continental keels on Earth requires not only that the keel be buoyant relative to normal sublithospheric mantle but a relatively high viscosity [10]. Thus, keel material is expected to be cold, depleted, and dehydrated. There is yet no evidence for a depleted, dehydrated region of the Martian mantle. Without seismology, our best hope for additional constraints on Martian crustal structure are thermobarometric studies of xenolith inclusions in lavas and/or discovery of kimberlites.

Since gravity on Mars is roughly one third of that on Earth, the growth time for EDC instabilities will be approximately three times as long on Mars as Earth. This implies that the velocities of EDC flow on Mars will be smaller than on Earth, hence the total amount of mantle cycled through the melt zone will be less than on Earth for the same given period of time. This works against viability of the small-scale instability idea.

2) Would this boundary have been likely to exist at the time of the formation of the dichotomy boundary? Cratering studies demonstrate that northern plains are similar in age to the southern hemisphere [8,9]. Thus, the dichotomy boundary is

an old feature. Numerical small-scale convection experiments show that an EDC instability can last for at least 50-100 million years, limited mostly by the erosion of the step in the boundary [1]. (This is highly dependent on the mechanical properties of the step boundary.) The EDC instability continuously draws new (unmelted) mantle material through the melting zone, and melting occurs dominantly by pressure release. This time period is reasonably consistent with the time period for the major phase of Tharsis volcanism. It is possible that a series of EDC type instabilities along the dichotomy boundary through time together form Tharsis rise. King and Anderson [1] estimated that an EDC instability could produce the volume of volcanic material observed at flood basalt provinces such as the Parana basalts of South America. Tharsis rise is 10-30 times the volume of volcanic material of typical flood basalt provinces on Earth. The very-short duration of flood basalt volcanic activity is problematic for the EDC mechanism; however, this does not appear to be the case for Tharsis rise. Given the age of the major phase of Tharsis volcanism, it seems highly improbable that if a small-scale instability was responsible for the formation of Tharsis, the instability remains active today.

Summary: The most intriguing aspect of a Tharsis-dichotomy connection is the spatial relationship. Not only does the Tharsis rise straddle the dichotomy boundary, it is located in the interior of a concave arc of the boundary. Thus small-scale instabilities from 5,000 km of arc-length along the boundary could potentially feed Tharsis volcanism. If an EDC existed and formed the volcanism comprising Tharsis rise in the Late-Noachian to Early-Hesperian period, it is unlikely that the same instability remains active today. If an EDC mechanism is responsible for the small, late-stages of volcanic activity, it is possible that it could be observable in the present areoid and topography. Figure 2 shows the residual areoid from degrees 5-60 after the best fitting isostatic areoid, in a least-squares sense, has been removed. The best fitting isostatic model has a crustal thickness of 110 km and a crustal density of 2800 kg/m^3. The result is relatively insensitive to whether we use degrees 5-8 as the low-end cut off. The zero km elevation line of the topography is plotted as a proxy for the crustal dichotomy. The linear relative areoid highs in the residual that parallel the dichotomy could represent mantle structures paralleling the crustal feature.

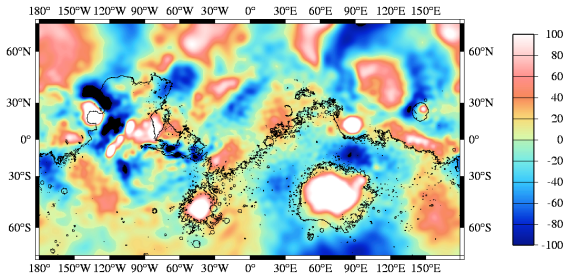

Figure 2. Spherical harmonic degrees 5-60 of the areoid where the best fitting isostatic areoid (crustal density 2800 kg/m^3, crustal thickness 100 km) has been removed. The black line is the zero contour of the topography, a proxy for the crustal dichotomy.

A number of factors appear to work against an EDC instability as the major source of Tharsis volcanism; however, given our limited knowledge of the thermo-chemical state of the Martian lithosphere it is not possible to rule out an EDC mechanism. More importantly, an EDC mechanism could easily explain the minor, late-stage volcanic activity associated with Tharsis and present day small-scale convection could have a signature in the Areoid.

Another interesting possibility is that the major phase of Tharsis volcanism could be related to a lower-crustal Rayleigh-Taylor type instability [11]. A similar mechanism has been proposed as the source of the Yellowstone-Newbury volcanism in the western US [12]. The most striking question that these mechanisms do not address is the same one that plagues the plume mechanism; why is there a single, long-lived volcanic feature on Mars?

References: [1] King S. D. and Anderson D. L. (1998) *Earth Planet. Sci. Lett., 160,* 289-296. [2] Vogt P. R. (1991) *Geology, 19,* 41-44. [3] King S. D. and Ritsema J. (2000) *Science, 290*, 1137-1140. [4] Kaula W. M. (1967) *Rev. Geophys., 5*, 83-107. [5] Hauck II S. A. and Phillips R. J. (2002) *JGR, 107,* 10.1029/201JE001801. [6] Harder H. and Christensen U. R. (1996) *Nature, 380,* 507-509. [7] Lowry A. R. and Zhong S. (2003) *JGR, 108,* 10.1029/2003JE002111. [8] Frey et al. (2002) *GRL, 29,* 10.1029/2001GL013832. [9] Solomon S. C. (2002) *Nature, 418,* 27-29. [10] Lenardic A. et al. (2003) *JGR, 108,* 10.1029/202JB0001859. [11] Jull M. and Kelemen P. B. (2001) *JGR, 106,* 6423-6446. [12] Humphreys et al. (2000) *GSA Today, 10(12),* 1-7.

MARS AND EARTH: TWO DICHOTOMIES – ONE CAUSE. G. G. Kochemasov. IGEM Russian Academy of Sciences, 35 Staromonetny, 119017 Moscow, Russia, kochem@igem.ru.

The wave planetology [1, 2, 3 and others] is based on this fundamental thesis: orbits make structures. It means that inertia-gravity forces arising in planetary bodies due to their movements in non-round (elliptical, parabolic) keplerian orbits with periodically changing curvatures and accelerations produce in planetary spheres oscillations. Having standing character and four directions (ortho- and diagonal) these oscillations (waves) interfere forming uplifting (+), subsiding (-) and neutral compensated (0) tectonic blocks. These blocks, naturally, are regularly disposed and their sizes depend on wavelengths. The longest fundamental wave 1 (long $2\pi R$, where R is a body radius) inevitably produces tectonic dichotomy (Fig. 1) with one hemisphere rising (+) and another falling (-). The rising (continental) hemisphere increases its planetary radius thus occupying larger space (surface) and tending to extend itself. That is why it is normally profoundly and intensively cracked (rifted) giving way up to deep-seated (mantle) melts; volcanoes, plateau flood basalts appear, intrusions fill weakness zones. The falling (oceanic) hemisphere diminishes its planetary radius thus occupying smaller space (surface) and tending to contract itself. That is why it is normally folded and extra material is pushed up (squeezed out), finds its way to the surface forming volcanoes and ridges. As all planetary bodies rotate, tectonically and hypsometrically different levels blocks (hemispheres) must regulate (equilibrate) their angular momenta: otherwise a globe will tend to fall to pieces (destroy itself). As the angular velocity of rotation of all blocks in one body is the same, the equilibration must be done by play between radii and densities. The subsiding blocks thus must be denser than the uplifting blocks. Our observations confirm this: at Earth oceans are basaltic and continents are on average andesitic. Mars also obeys this law: the northern lowlands are Fe-basaltic and the southern highlands are andesitic at least at the dichotomy boundary ('Pathfinder") and must be else less dense further south (we proposed albitites, syenites and granites as candidates to these low density rocks [3, 4, 5, 6 and others]).

The density contrast between highlands and lowlands at Earth is about 0.25 g/cm^3 , at Mars this contrast must be even higher because the martian wave tectonics is sharper (coarser) and produces relatively larger blocks with higher relief range [4]. The martian lowlands, indeed, are denser than the terrestrial ones (Fe-basalts against tholeiites). The recent martian lander's data published in Internet show that highlands layered rocks (by the way, such thin layering is typical of terrestrial nepheline syenites, for an example, Lovozero massif at Kola peninsula [7, 8]) covered by crusts of sulphates, chlorides, bromides are Si, Al, alkali – rich. High Cl and sulphur oxides are typical for syenites [7, 8]. Mg/Fe and Al/Ca in martian analyses are high and there is a sharp increase of them from lowlands to highlands indicating a pronounced global chemical fractionation (no more dull entirely basaltic Mars !). Global Si and Fe distribution according to the Odyssey gamma-spectrometry means that the southern highlands are Si-rich and the northern lowlands Fe-rich. The global gravity [9] also shows that the southern buckling hemisphere is built of relatively light (not dense) lithologies (albedo supports this conclusion).

So, the E-W and S-N dichotomies of Earth and Mars, where are opposed uplifting deeply rifted highlands and subsiding markedly ridged (folded) lowlands, are identical wave features of the first order. In both cases the lowlands (the primary oceans) occupy ~ 1/3 of the whole global surface, that is an another indication of waves involved (Fig. 1).

According to the wave theory the first harmonic – wave 1 typically is adorned by overtones. The first overtone – wave 2 is the most pronounced and shows itself by separate block-sectors - continents and separating them secondary oceans. At Earth the eastern continental hemisphere (segment) is composed of continents and oceans (sectors), the western oceanic hemisphere (segment) of oceanic plateaus and depressions (sectors). The sectoral features of two hemispheres are antipodean (i. g., Africa and East-Pacific depression). The martian segments also are composed of different level sectors. The most pronounced on the southern highland segment are two depressions – Hellas planitia and Argyre planitia. They have their anti-counterparts on the northern lowland segment – antipodean but uplifted features. Hellas is antipodean to appearing at high oceanic latitudes "continental" block of Alba patera and Tempe terra. Argyre is nearly antepodean to lonely protruding oceanic floors Elysium planum (together with its northern extension – Phlegra montes) (Fig. 2). Isidis planitia is antepodean to the complex of three plana: Solis, Syria, Sinai. And so on…

Structural similarities of two planets completely differing in size, mass and average density could be continued and found also in other planetary bodies including small ones – asteroids and the boss – Sun (aster), more precisely, its photosphere [10, 11]. These structural regularities allowed us to generalize them in four theorems of planetary tectonics [12]: 1. Celestial bodies are dichotomic; 2. Celestial bodies are sectoral; 3. Celestial bodies are granular; 4. Angular momenta of different level blocks tend to be equal.

Two more remarks. 1) Why dichotomies of Mars and Earth are differently oriented (S-N & E-W)? Because in the interference process take place waves of 4 directions; they have several possibilities to combine, to superimpose on each other forming "+" and "-" at different sides. 2) Why the dichotomy boundary is so sharp? Because waves we deal with are quantum-mechanical ones that means they do not have smooth sinusoidal

transitions between phases: there is discrete sharp transition between "+" and "-" (remember sharp boundaries between continents and oceans on Earth).

References: [1] Kochemasov G. G. (1994) 20th Russian-American microsymposium on planetology. Abstr., Moscow, Vernadsky Inst., 46-47; **[2]** Kochemasov G. G. (1998) Proceedings of international symposium on new concepts in global tectonics ('98 TSUKUBA), Tsukuba, Japan, Nov. 1998, 144-147; **[3]** Kochemasov G. G. (1999) The Fifth International Conference on Mars, July 18-23, 1999, Pasadena, California. Abstr. # 6034. LPI contribution # 972. LPI, Houston, (CD-ROM); **[4]** Kochemasov G. G. (1995) Golombek M.P., Edgett K.S., Rice J.W. Jr. (Eds). Mars Pathfinder Landing Site Workshop II: Characteristics of the Ares Vallis Region and Field trips to the Channeled Scabland, Washington. LPI Tech. Rpt. 95-01. Pt.1.LPI, Houston, 1995, 63 pp.; **[5]** Kochemasov G. G. (1997) Annales Geophysicae, Suppl. III to Vol. 15, Pt. III, 767; **[6]** Kochemasov G. G. (1998) Annales Geophysicae, Suppl. III to vol. 16, Pt. III, 1027; **[7]** Kochemasov G. G. (2001) Eleventh Annual V. M. Goldschmidt Conference. Hot Springs, Virginia, USA. Abstr. # 3070. LPI, Houston, 2001, (CD-ROM); **[8]** Kochemasov G. G. (2001) Field Trip and Workshop on the Martian Highlands and Mojave Desert Analogs, Las Vegas, Nevada, and Barstow, California, Oct. 20-27, 2001. LPI contribution # 1101, LPI, Houston, 35-36; **[9]** Smith D. E., Sjogren W. L., Tyler G. L. et al. (1999) Science, v. 286, 94-97; **[10]** Kochemasov G. G. (2003) 38th microsymposium on comparative planetology, Abstr., Moscow, Vernadsky Inst., (CD-ROM); **[11]** Kochemasov G. G. (2004) Lunar and Planetary Science XXXV, 35th LPSC, Houston, March 15-19, 2004, Abstr. # 1041, (CD-ROM); **[12]** Kochemasov G. G. (1999) Geophys. Res. Abstr., v. 1, # 3, 700; **[13]** Zuber M. T., Solomon S. C., Phillips R. J., Smith D. E. et al. (2000) Science, v. 287, # 5459, 1788-1793.

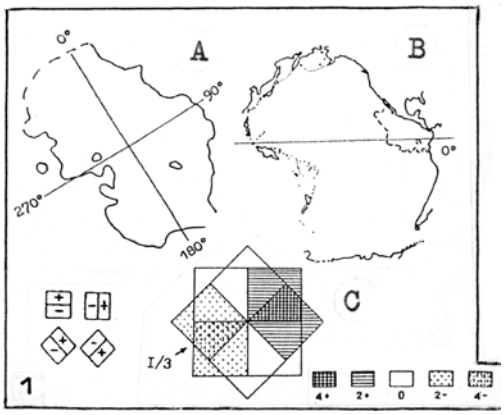

Fig. 1. Identical formation of Mars' and Earth's tectonic dichotomy: a model of wave interference. **A**-Vastitas Borealis of Mars. Crustal thickness inside the contour is less than 50 km [13] (as viewed from inside the globe what makes the contour mirrored). **B**- Pacific basin. **C**- Flat geometric model of wave interference (4 wave directions). One needs mentally to wrap up it around the globe.

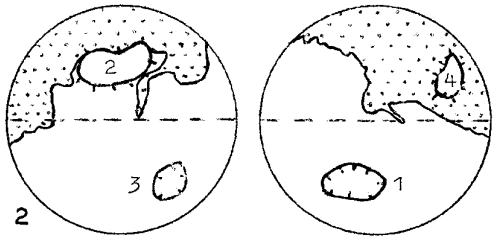

Fig. 2. Martian hemispheres with dichotomy boundary. Antipodality of Hellas (1) to Alba patera and Tempe terra (2) and Argyre (3) to Elysium planum with Phlegra montes (4).

DEPTH-DEPENDENT RHEOLOGY AND THE WAVELENGTH OF MANTLE CONVECTION WITH APPLICATION TO MARS. A. Lenardic, *Department of Earth Science, Rice University, Houston, Texas, (adrian@esci.rice.edu)*, M.A. Richards, *Department of Earth and Planetary Science, University of California, Berkeley, California*, F.H. Busse, *Institute of Physics, University of Bayreuth, Bayreuth, Germany*, S.J.S. Morris, *Department of Mechanical Engineering, University of California, Berkeley, California*.

Abstract: Numerical simulations have shown that depth-dependent viscosity can increase the wavelength of mantle convection. The physical mechanism behind this observation and, by association, its robustness remain to be fully elucidated. Towards this end, we develop theoretical heat flow scalings for a convecting fluid layer with depth-dependent viscosity. Bottom and internally heated end-members are considered. For the former, the viscosity structure consists of a high viscosity central region bounded from above and below by horizontal low viscosity channels. For internally heated cases, only a surface low viscosity channel is present. The theoretical scalings show how depth-dependent rheology lowers the lateral dissipation associated with convective cells. This allows longer aspect ratio cells to form as the viscosity contrast between the channels and the central region is increased. The maximum cell extent is determined by the condition that the pressure gradients that drive lateral flow in the channels do not become so large as to inhibit vertical flow into the channels. Scaling predictions compare favorably to results of numerical simulations at low to moderate Rayleigh numbers. As the Rayleigh number driving convection is increased, time-dependence sets in in the form of small scale boundary layer instabilities. This increases lateral dissipation within the channels and the maximum cell extent decreases as a result. Internally heated simulations show that a near surface high viscosity layer, a lithosphere analog, can suppress these small scale instabilities. This allows a low viscosity channel to maintain large aspect ratio cells at high Rayleigh numbers.

Introduction: Several models for the formation of the Martian Hemispheric Dichotomy invoke long wavelength mantle convection [1,2,3]. Understanding the physical mechanisms by which long wavelength flow can be generated and maintained is crucial to evaluating the physical plausibility of such models under parameter conditions pertinent to Mars. Numerical simulations have been used to argue that depth-dependent viscosity can generate long wavelength flow within a convecting mantle [2,4]. However, numerical simulations have also been used to argue that depth-dependent viscosity will not be effective at generating long wavelength flow at the high degrees of convective vigor that characterize the Earths present day mantle and the Martian mantle at the time the dichotomy formed [5]. Clearly the simulations are mapping different dynamic regimes within the full parameter space of the system. To augment and extend the numerical work done to date, we have developed a scaling theory that explores the heat transfer properties of a convecting layer with depth-dependent rheology. The theory provides an efficient way to map regime transitions. It also provides physical insight into the observation that numerical simulations with depth-dependent rheology can generate long wavelength flow, i.e., it can isolate the physical reason why this is so and also determine the specific conditions required.

Analysis: Although the criteria that determines the selection of convective planforms within a thermally convecting fluid is not generally understood [6], it is agreed that it is lateral dissipation that principally limits the formation of large aspect ratio cells [7]. We develop a boundary layer theory based on the key assumption that the presence of horizontal regions of low viscosity (e.g. the Earth's asthenosphere, a low viscosity upper Martian mantle) within a convecting layer allow lateral flow to become channelized within the low viscosity regions [8]. The analysis shows that channelization lowers the lateral dissipation in fully developed, large amplitude convective flow systems heated from below or from within. This shifts the limit on the maximum cell extent that is energetically favorable. That is, with depth-dependent viscosity, the cell wavelength that is most effective at transporting heat is longer than for the isoviscous case. Although this does not guarantee that long cells will form preferentially to shorter cells, it does show how depth-dependent viscosity can make this more likely. Theory predictions for maximum cell wavelength as a function of viscosity variations, channel thicknesses, and convective vigor compare favorable to the results of numerical simulations. The theory explains why increased Rayleigh numbers can cause the wavelength to shift back to shorter length scales and suggests that the presence of a high viscosity, active lithosphere can offset this shift. The theory also predicts the counterintuitive results that long wavelength cells can increase the cooling rate of a planet and that thinner low viscosity channels can also increase the cooling rate. Both predictions are confirmed via full numerical simulations.

Discussion: For application to Mars, our theory suggests that: 1) Horizontal regions of low viscosity can lead to long wavelength mantle flow by lowering the lateral dissipation within the mantle; 2) The viscosity contrast between low viscosity regions and the bulk mantle must approach 1000 to generate wavelengths at the scale of a degree 1 mantle convection pattern; 3) Internal heating can favor long wavelength flow by decreasing the lateral dissipation associated with a hot lower thermal boundary layer; 4) For long wavelength flow to have occurred at the high degrees of convective vigor during Dichotomy formation, the Martian lithosphere needed to be active as opposed to stagnant; 5) If long wavelength flow did occur it could have helped to cool Mars at a faster rate than it would have in the absence of long wavelength flow; 5) Very thin low viscosity regions can have a significant effect on mantle cooling rate, i.e., potentially thinner than can be detected via geoid and topography analysis [9].

[1] McGill and Dimitriou, *Geology, 28*, 391-394, 1990. [2] Zhong and Zuber, *Earth Planet. Sci. Lett., 189*, 75-84, 2001.

[3] Lenardic et al., *J. Geophys. Res., 109*, 10.1029/2003JE002172, 2004. [4] Bunge et al., *Nature, 379*, 436-438, 1996. [5] Tackley, *Geophys. Res. Lett., 23*, 1985-1988, 1996. [6] Ahlers, *25 Years of Nonequilibrium Statistical Mechanics*, 91-124, Springer-Verlag, Berlin, 1995. [7] Busse, *Hyrdodynamic Instabilities and the Transition to Turbulence*, 97-137, Springer-Verlag, Berlin, 1985. [8] Lenardic et al., *Geophys. I. Int.*, Submitted. [9] Thorval and Richards *Geophysical J. Int., 131*, 1-8, 1997.